

# VASP: DFT and Beyond

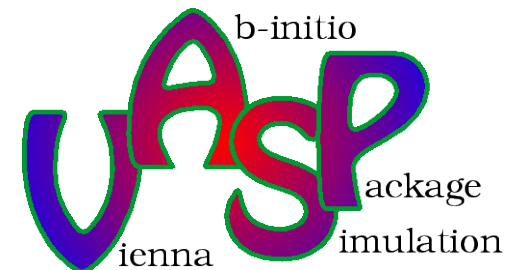
Martijn Marsman, and Georg Kresse

Computational Materials Physics, Faculty of Physics, University Vienna,  
Vienna, Austria

Theory and Computation for Interface Science and Catalysis,  
3-7th November 2014, Brookhaven National Laboratories, USA



universität  
wien



# Overview

- Past
  - The Workhorse: DFT
  - Efficient and stable algorithms
  - PAW potential database
- Present
  - Beyond DFT, and beyond the groundstate:  
Hybrid functionals, linear response, GW, BSE, ACFDT(RPA)
- Future
  - Near future: cubic-scaling-RPA (ACFDT & GW)
  - ...

# The Workhorse: Kohn-Sham DFT

$$\hat{H}\Psi(\mathbf{r}_1, \dots, \mathbf{r}_N) = E\Psi(\mathbf{r}_1, \dots, \mathbf{r}_N)$$

$$\Psi(\mathbf{r}_1, \dots, \mathbf{r}_N) \quad (\#\text{grid points})^N$$

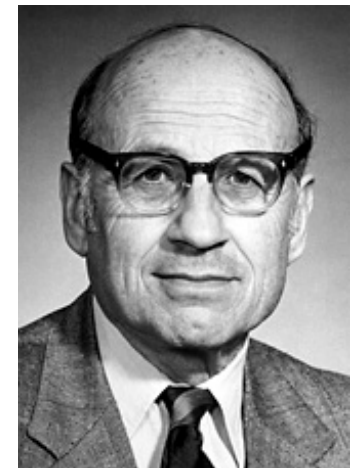
5 electrons on a 10×10×10 grid ~ 10 PetaBytes



$$\Psi(\mathbf{r}_1, \dots, \mathbf{r}_N) = \prod_i^N \psi_i(\mathbf{r}_i) \quad \rho(\mathbf{r}) = \sum_i^N |\psi_i(\mathbf{r})|^2$$

$$E[\rho] = T_s[\{\psi_i[\rho]\}] + E_H[\rho] + E_{xc}[\rho] + E_Z[\rho] + U[Z]$$

$$\left(-\frac{1}{2}\Delta + V_Z(\mathbf{r}) + V_H[\rho](\mathbf{r}) + V_{xc}[\rho](\mathbf{r})\right)\psi_i(\mathbf{r}) = \epsilon_i\psi_i(\mathbf{r})$$



$E_{xc}[\rho] = ???$      $V_{xc}[\rho](\mathbf{r}) = ???$     → Approximations: LDA, PBE, ...

# The Self-Consistency Cycle

$$\mathbf{H} = \langle \mathbf{G} | \hat{H}[\rho] | \mathbf{G}' \rangle \rightarrow \text{diagonalize } \mathbf{H} \rightarrow \{\psi_i, \epsilon_i\} \quad i = 1, \dots, N_{\text{FFT}}$$
$$\rho_0 \rightarrow \mathbf{H}_0 \rightarrow \rho' \rightarrow \rho_1 = f(\rho_0, \rho') \rightarrow \mathbf{H}_1 \rightarrow \dots$$

- In practice:

Iterative matrix  
diagonalization

blocked-Davidson

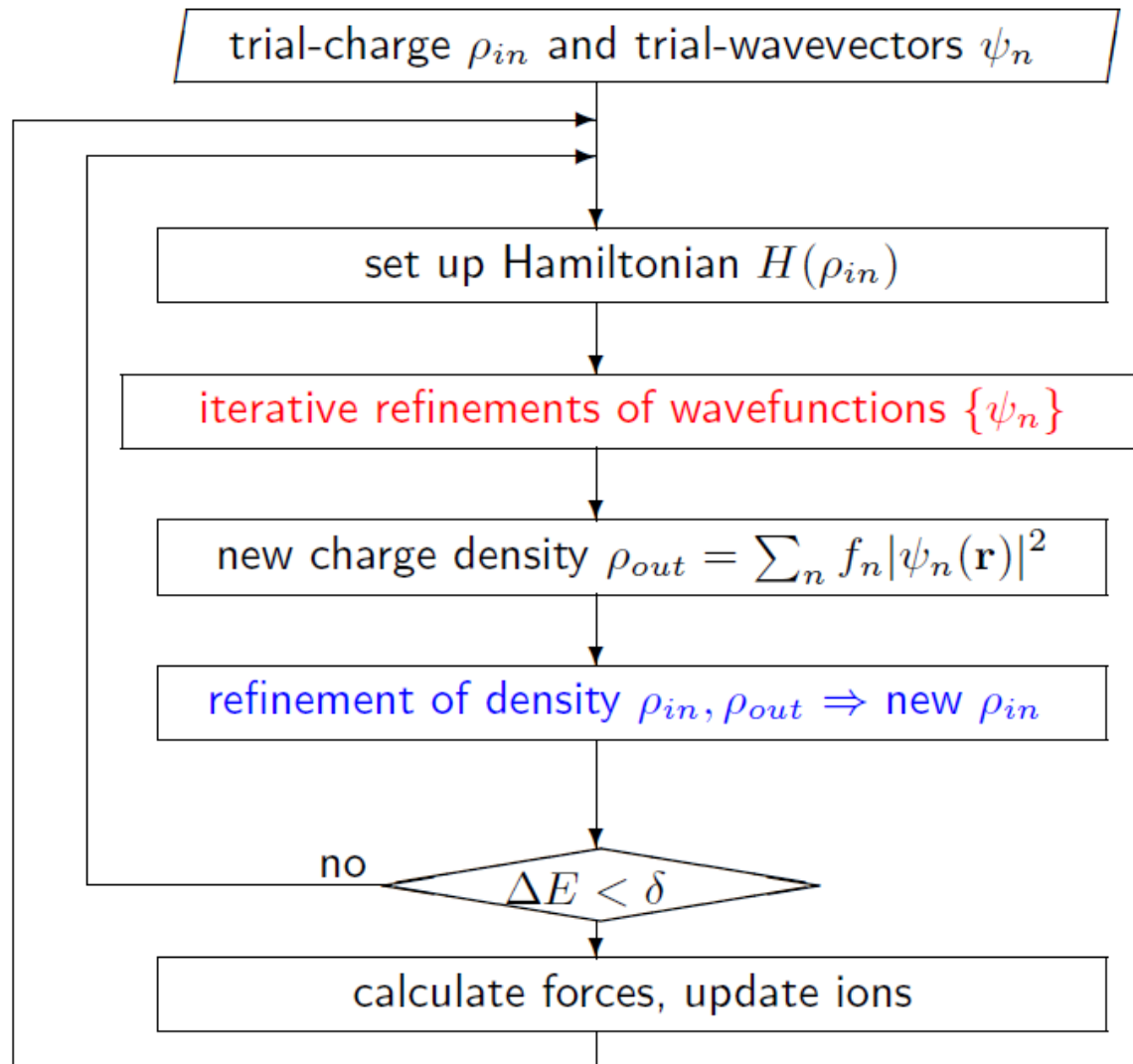
RMM-DIIS

Charge density mixing

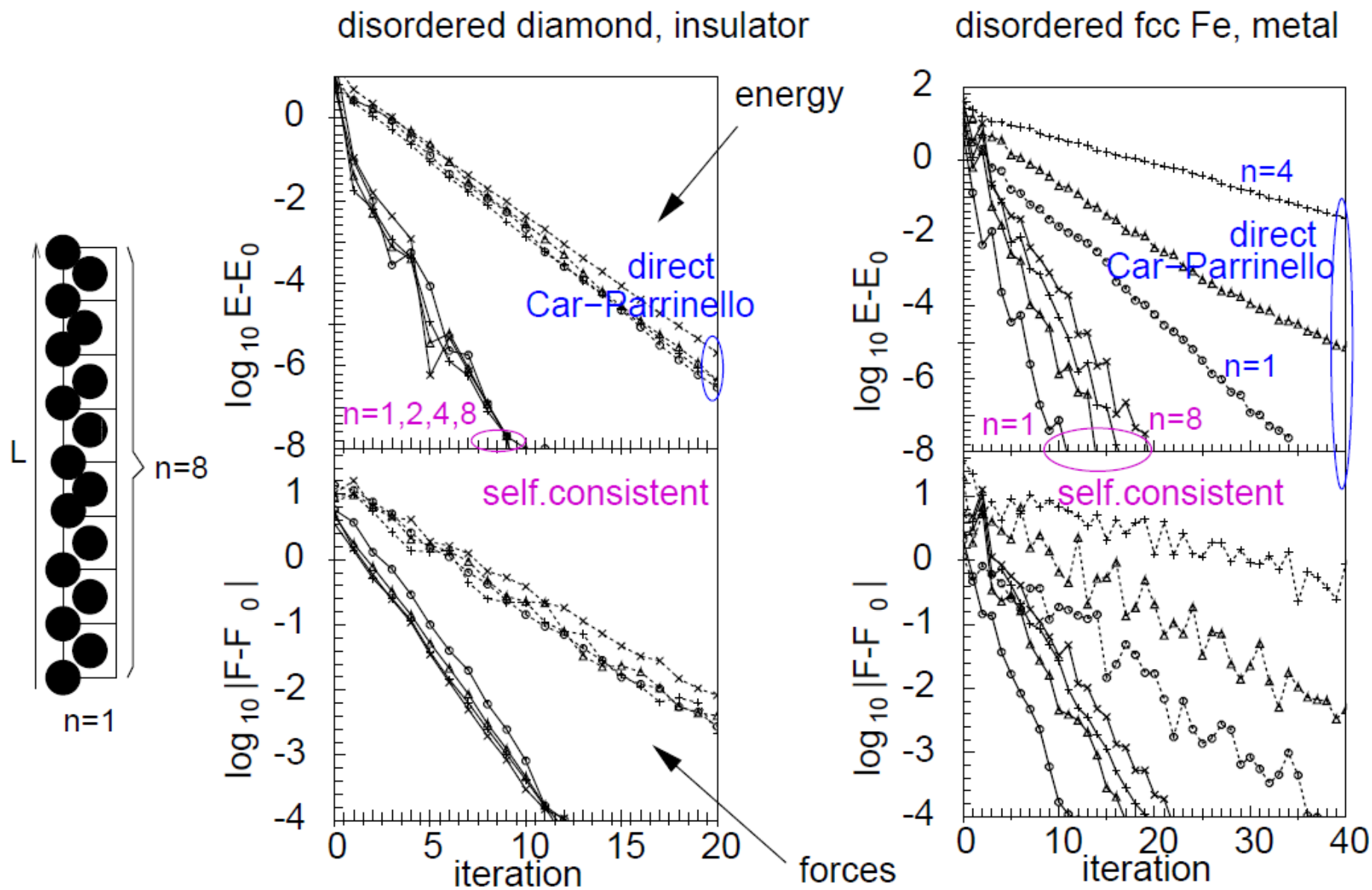
Broyden mixer

Orthonormalization

(bottleneck)



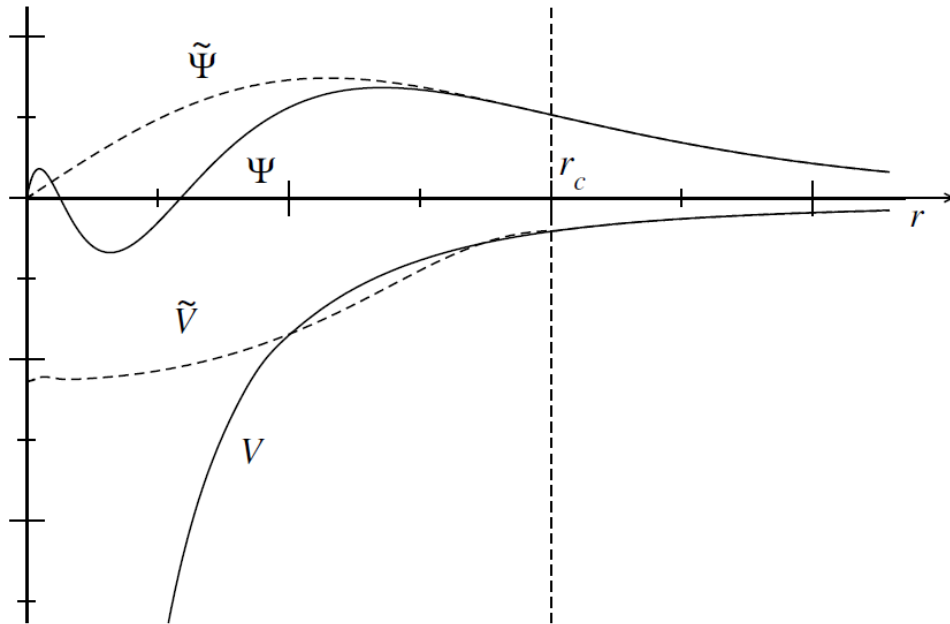
# Fast, robust, and unchanged since 1995



G. Kresse and J. Furthmüller, PRB 54, 11169 (1996)

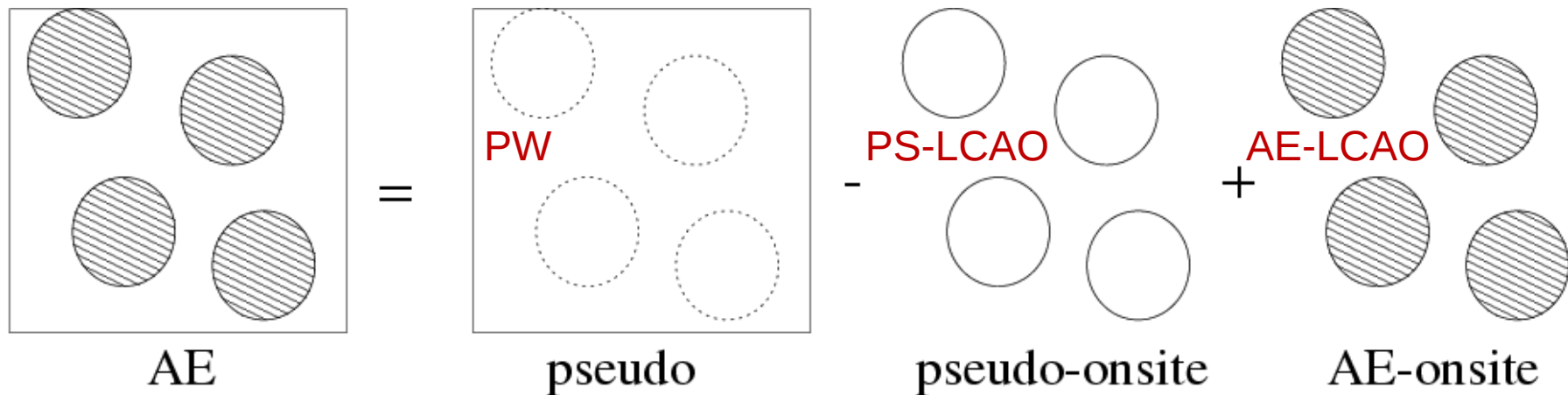
# Pseudopotentials & the PAW method

P. Blöchl, PRB 50, 17953 (1994), G. Kresse *et al.*, PRB 59, 1758 (1998)

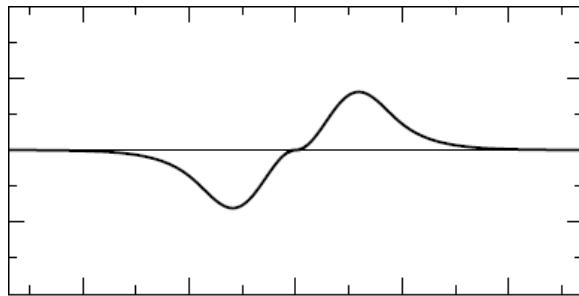


- Full potential (“all-electron” method)
- Frozen-core approximation: but core-valence interaction is treated at the same level as valence-valence.
- Pseudo wave function expressed in plane waves
- LCAO correction inside atom-centered spheres

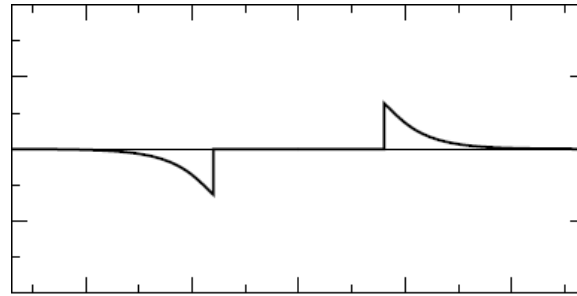
$$|\psi_n\rangle = |\tilde{\psi}_n\rangle + \sum_i (|\phi_i\rangle - |\tilde{\phi}_i\rangle) \langle \tilde{p}_i | \tilde{\psi}_n \rangle$$



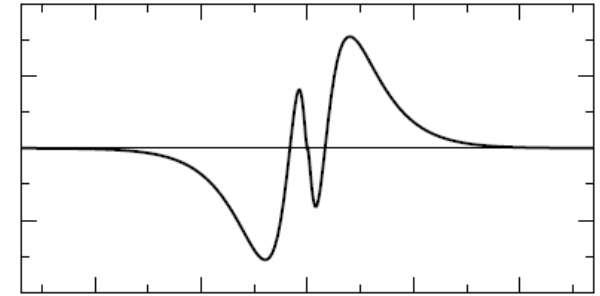
# The PAW method (cont.)



$$|\tilde{\psi}_n\rangle$$

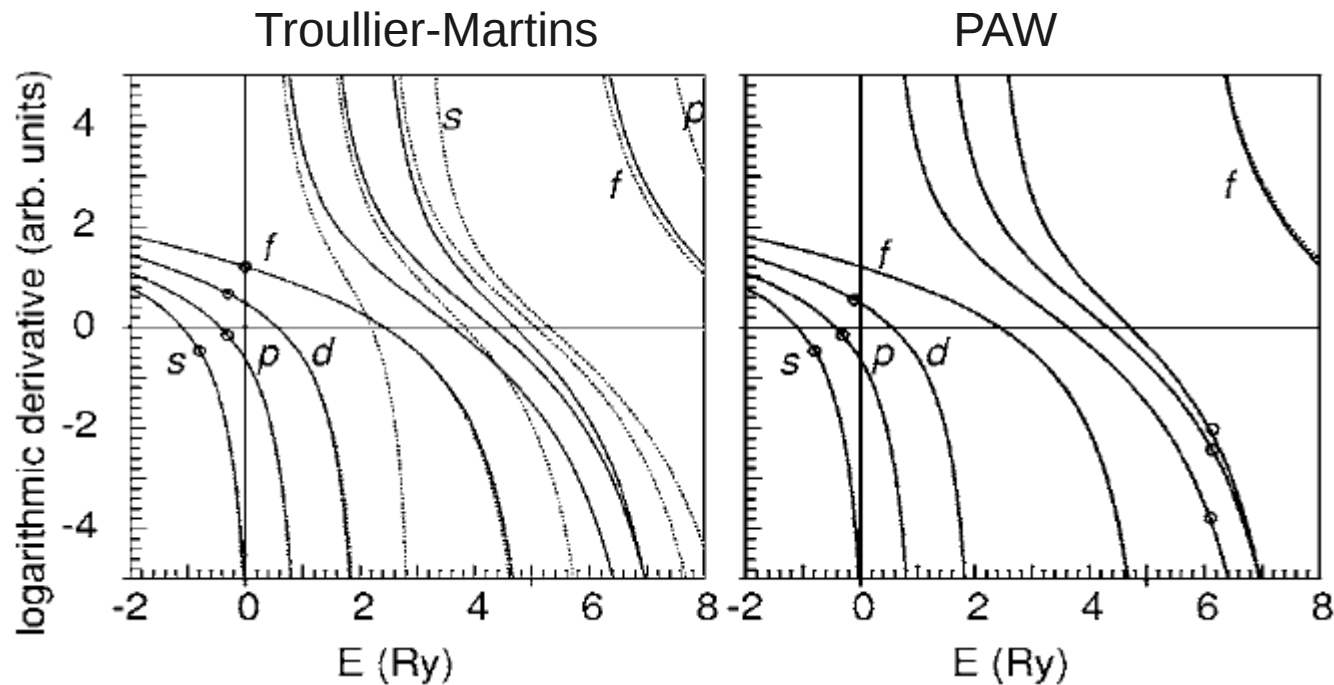


$$|\tilde{\psi}_n\rangle - \sum_i |\tilde{\phi}_i\rangle \langle \tilde{p}_i | \tilde{\psi}_n\rangle$$



$$|\tilde{\psi}_n\rangle - \sum_i |\tilde{\phi}_i\rangle \langle \tilde{p}_i | \tilde{\psi}_n\rangle + \sum_i |\phi_i\rangle \langle \tilde{p}_i | \tilde{\psi}_n\rangle$$

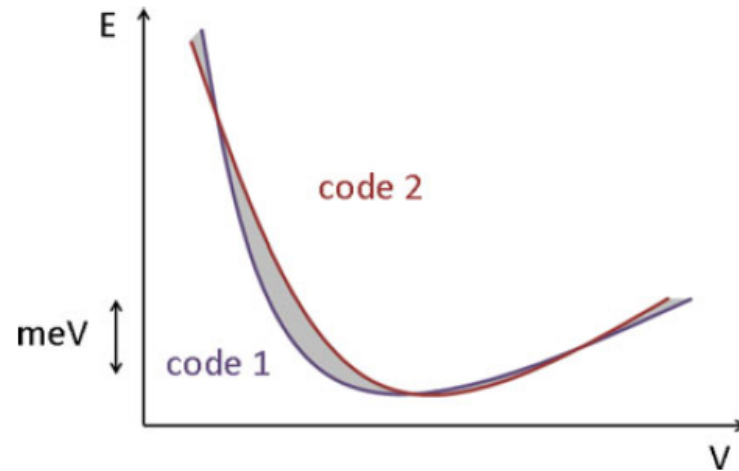
Si scattering properties



# $\Delta$ -evaluation (PAW vs. FLAPW)

K. Lejaeghere *et al.*, Critical Reviews in Solid State and Materials Sciences 39,1 (2014)

$$\Delta = \left\langle \sqrt{\frac{\int \Delta E^2(V) dV}{\Delta V}} \right\rangle$$



H																	He				
0,1																	0,0				
Li	Be															B	C	N	O	F	Ne
0,1	0,2															0,3	1,1	0,5	0,4	0,1	0,1
Na	Mg															Al	Si	P	S	Cl	Ar
0,7	0,5															0,1	0,1	1,7	0,3	1,4	0,0
K	Ca	Sc	Ti	V	Cr	Mn	Fe	Co	Ni	Cu	Zn	Ga	Ge	As	Se	Br	Kr				
0,1	0,5	0,4	0,7	1,0	0,8	0,5	0,6	1,9	0,3	1,8	1,2	0,7	0,4	1,2	0,7	0,1	0,1				
Rb	Sr	Y	Zr	Nb	Mo	Tc	Ru	Rh	Pd	Ag	Cd	In	Sn	Sb	Te	I	Xe				
0,1	0,1	0,6	0,5	0,6	2,4	1,4	0,3	0,7	0,5	0,2	3,2	0,3	0,1	0,4	0,2	0,4	0,1				
Cs	Ba	Lu	Hf	Ta	W	Re	Os	Ir	Pt	Au	Hg	Tl	Pb	Bi	Po	At	Rn				
0,0	0,8	3,5	2,0	0,4	1,0	2,1	0,8	1,4	1,6	0,4	1,0	0,2	0,1	0,1	0,6		0,0				

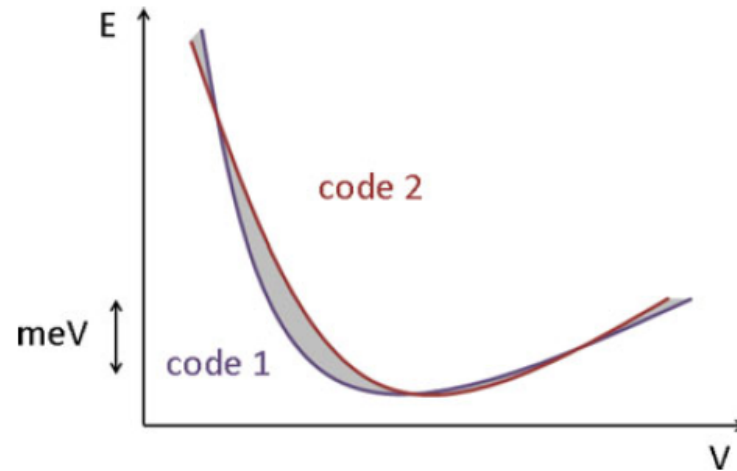
$\Delta(\text{PAW})_{(\text{VASP})} = 0.7 \text{ meV/atom}$

N.B.  $\Delta = 0.7 \text{ meV/atom}$ , and not  $1.9 \text{ meV/atom}$  (as published in Crit. Rev.)

# $\Delta$ -evaluation (PAW vs. FLAPW)

K. Lejaeghere *et al.*, Critical Reviews in Solid State and Materials Sciences 39,1 (2014)

$$\Delta = \left\langle \sqrt{\frac{\int \Delta E^2(V) dV}{\Delta V}} \right\rangle$$



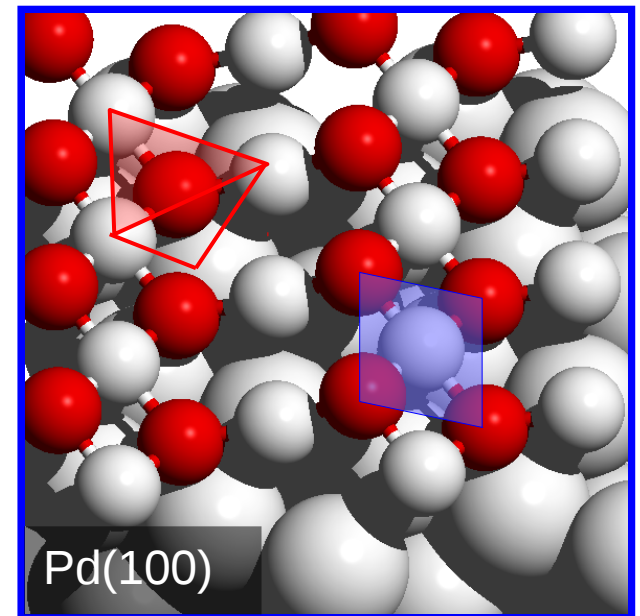
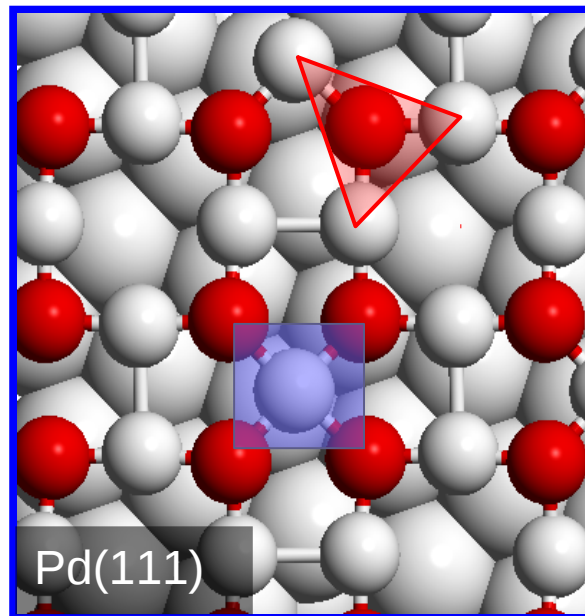
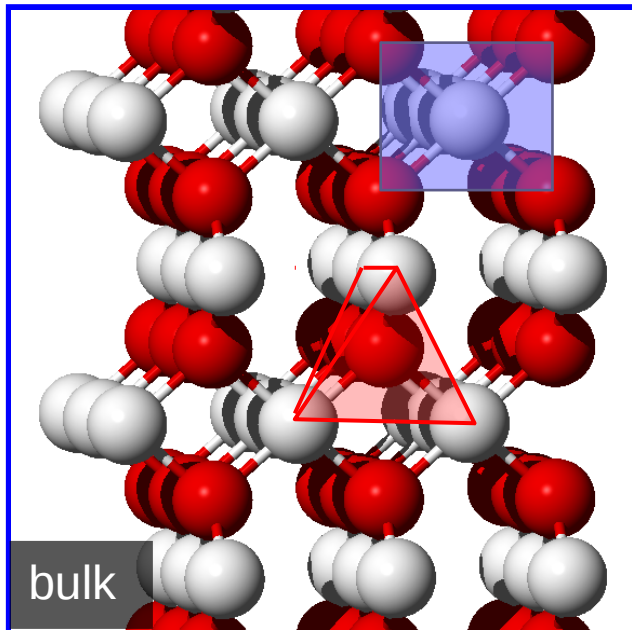
H																	He				
0,0																	0,0				
Li	Be															B	C	N	O	F	Ne
0,1	0,5															0,2	0,2	0,7	0,1	0,1	0,1
Na	Mg															Al	Si	P	S	Cl	Ar
0,4	0,0															0,3	0,1	0,0	0,2	0,0	0,1
K	Ca	Sc	Ti	V	Cr	Mn	Fe	Co	Ni	Cu	Zn	Ga	Ge	As	Se	Br	Kr				
0,1	0,4	0,3	0,3	0,1	0,8	0,1	0,1	0,2	0,8	0,5	0,6	0,8	0,7	0,8	0,4	0,2	0,1				
Rb	Sr	Y	Zr	Nb	Mo	Tc	Ru	Rh	Pd	Ag	Cd	In	Sn	Sb	Te	I	Xe				
0,1	0,2	0,5	0,4	0,2	0,9	0,1	0,2	0,3	0,4	0,3	2,5	0,2	0,2	0,5	0,9	0,9	0,1				
Cs	Ba	Lu	Hf	Ta	W	Re	Os	Ir	Pt	Au	Hg	Tl	Pb	Bi	Po	At	Rn				
0,1	0,3	3,5	1,7	0,8	1,2	0,9	0,5	0,8	0,3	0,1	1,0	0,2	0,1	0,5	0,6		0,0				

$\Delta(\text{PAW})_{(\text{VASP})} = 0.4 \text{ meV/atom}$

And the very best we can do (with reworked \*\_GW potentials)

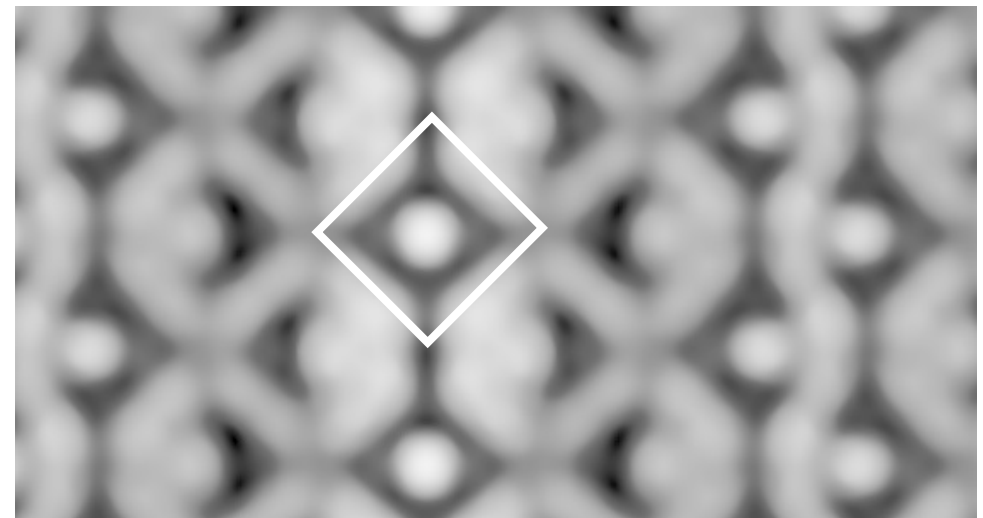
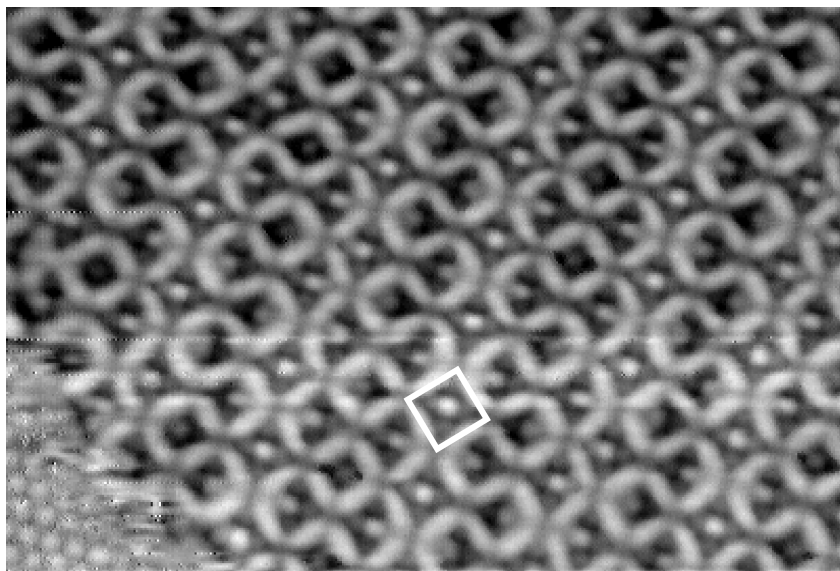
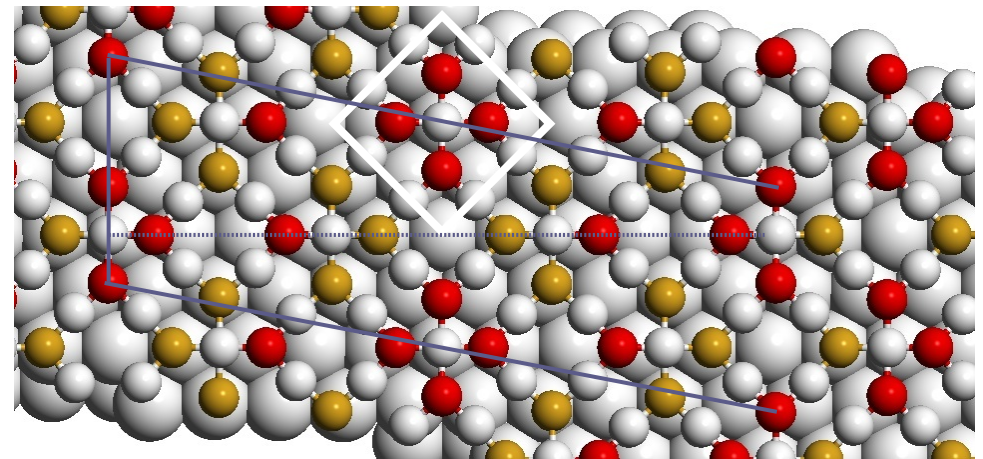
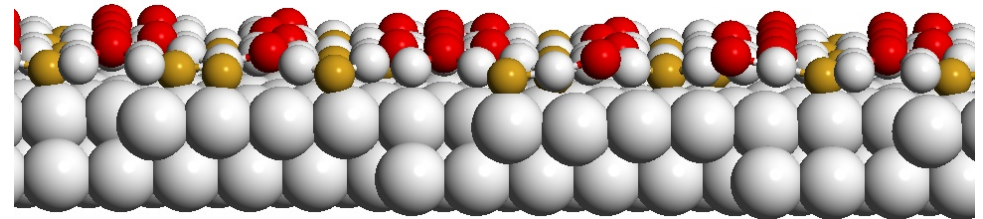
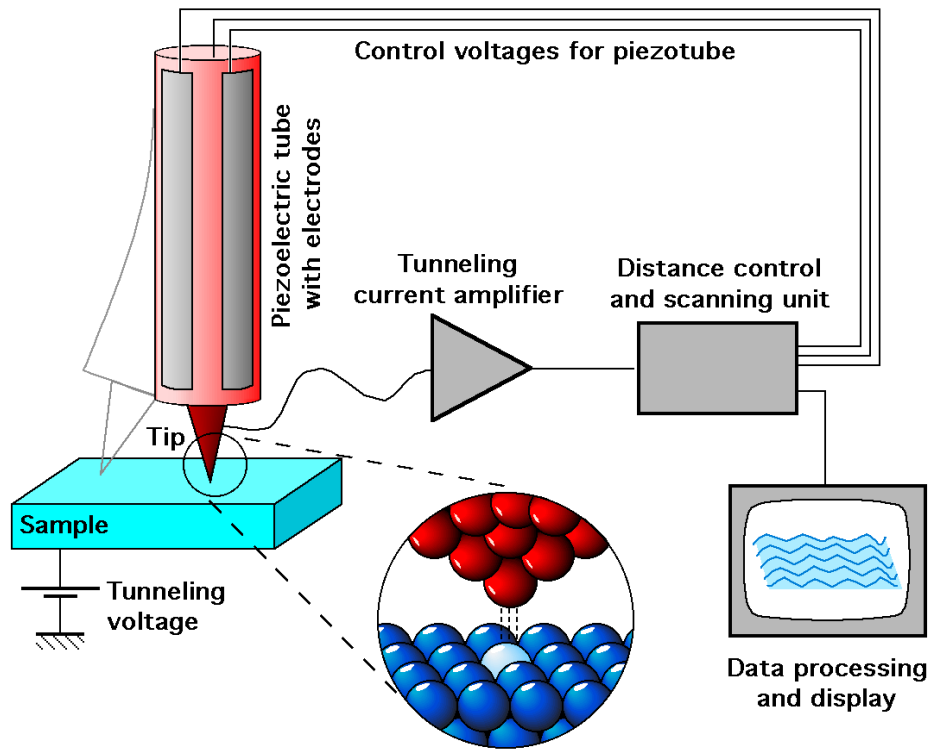
# Ultrathin PdO on Pd

- Complex reconstructions:
  - Different from bulk oxide
  - Not a straightforward continuation of the substrate
  - Bulk building blocks rearranged in new ways



# Ultrathin PdO layer on Pd(111): STM

Lundgren *et al.*, PRL 88, 246101 (2002)



# Core level shifts

Lundgren *et al.*, PRL 88, 246101 (2002)

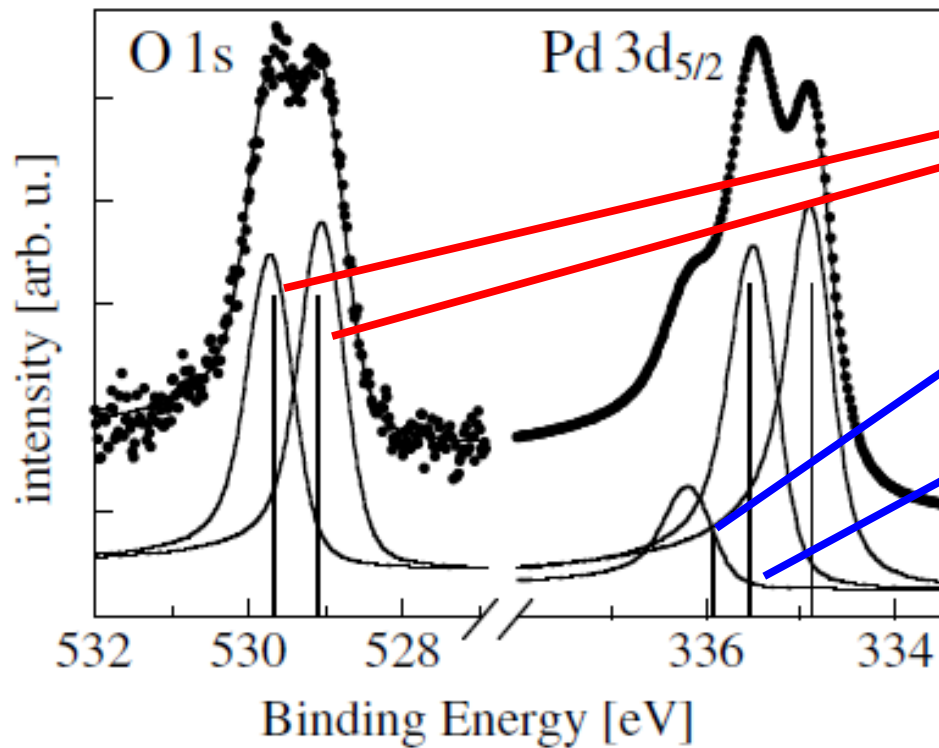
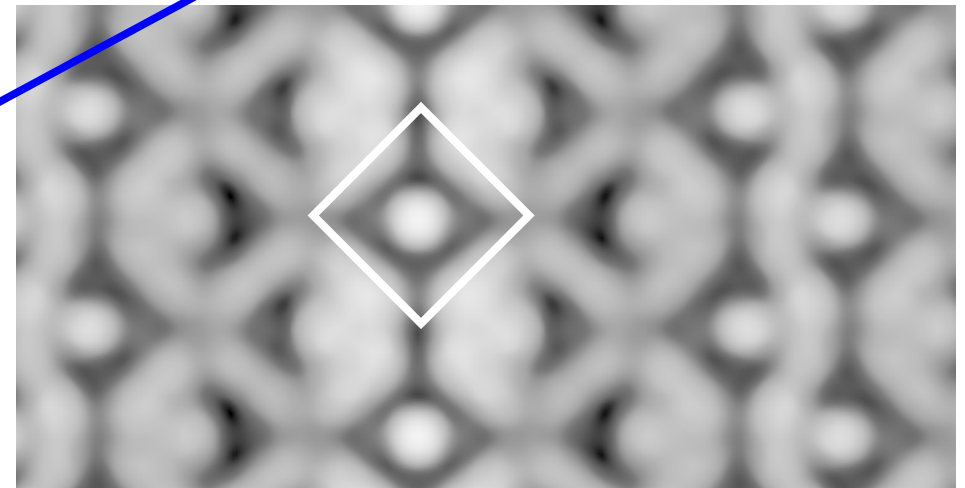
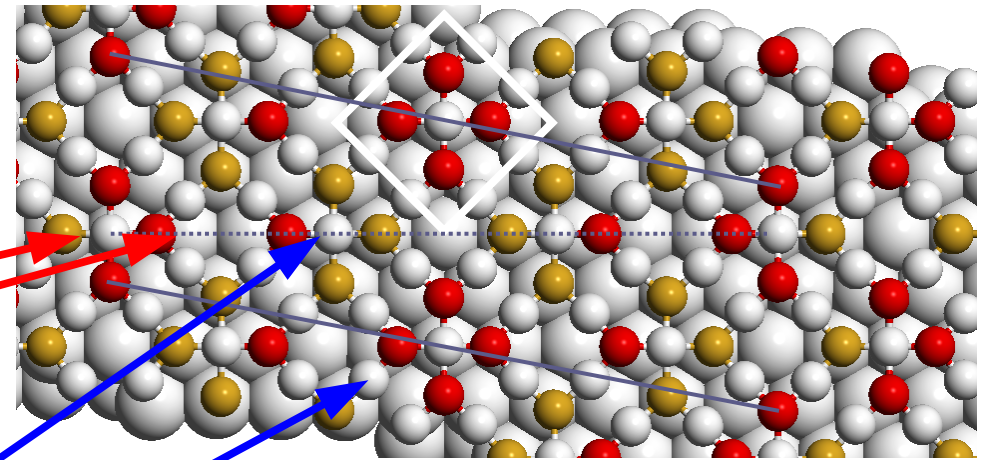
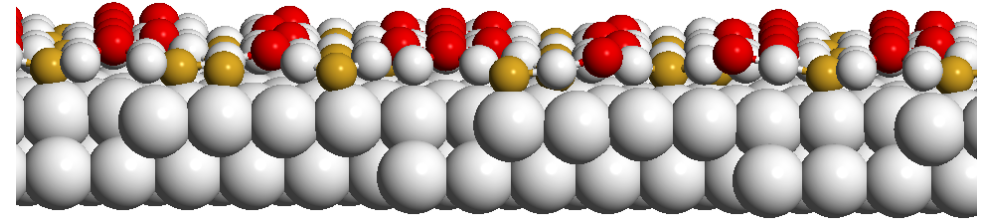
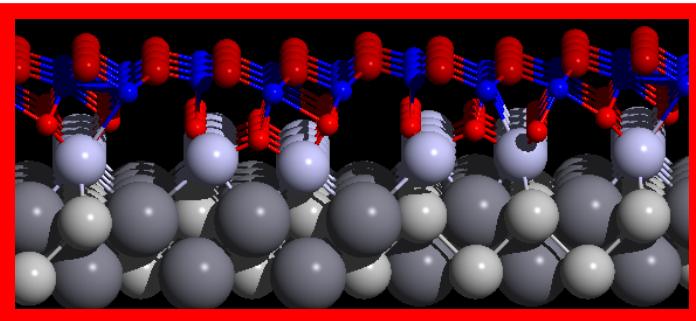
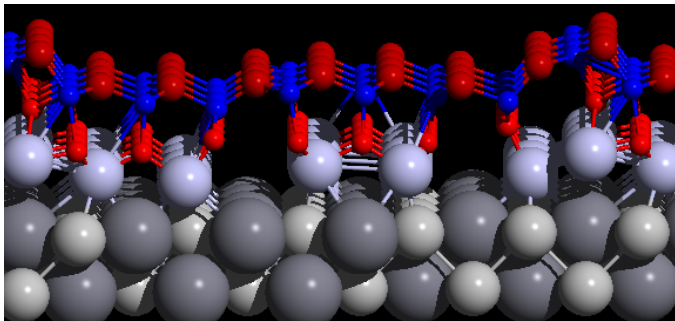
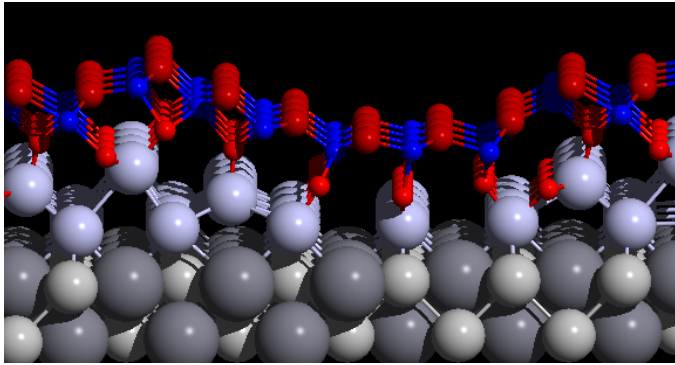
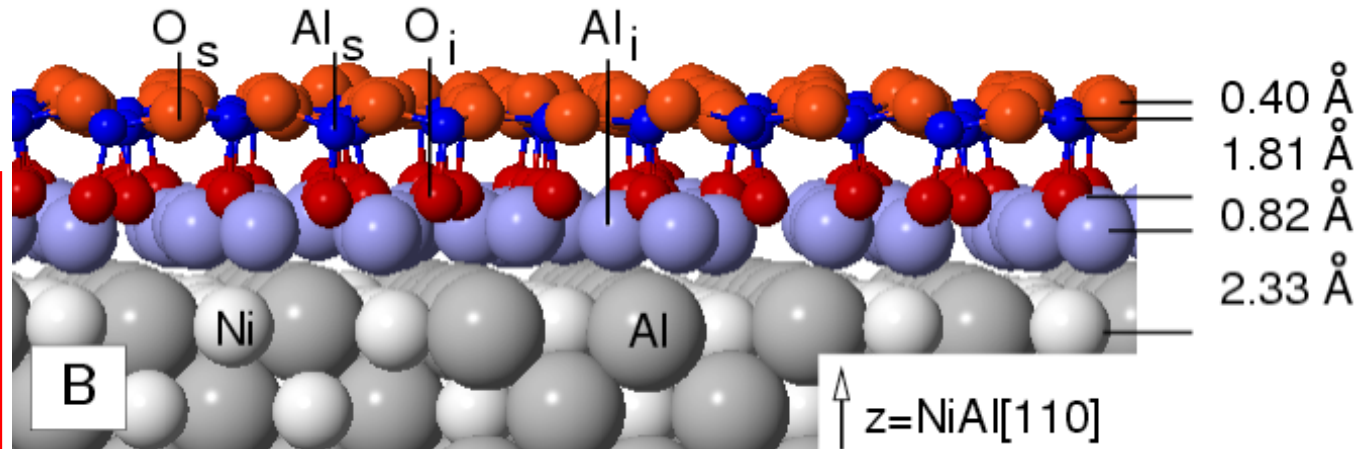


FIG. 3. HRCL spectra from the O 1s and the Pd 3d<sub>5/2</sub> levels of the surface oxide [21]. Calculated binding energies (averages over groups of atoms with equivalent sites) are indicated as vertical lines.

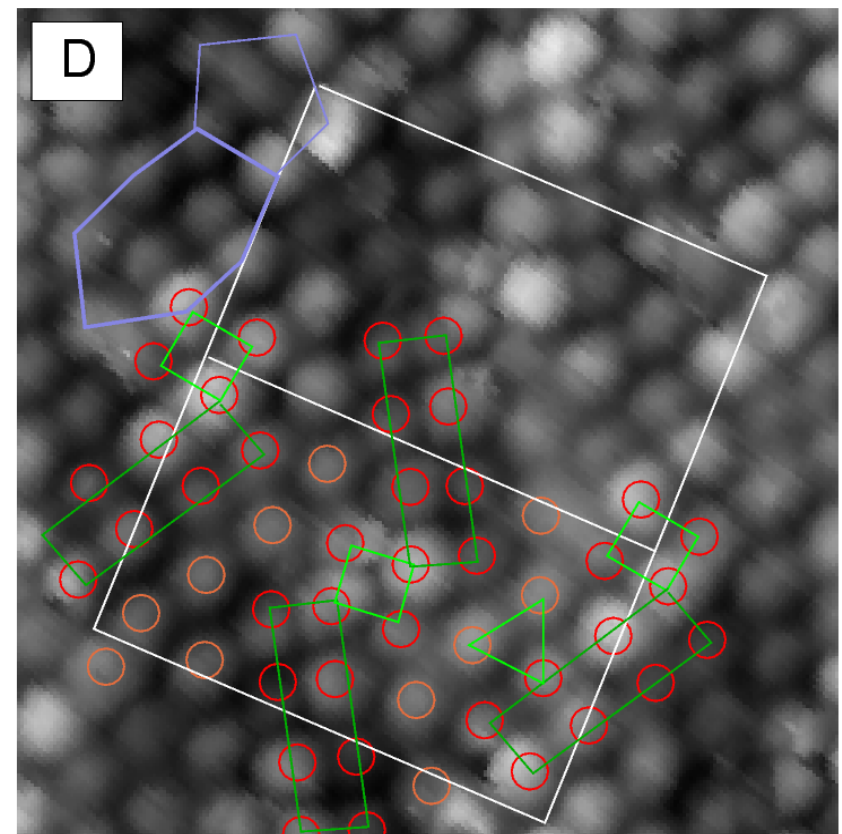
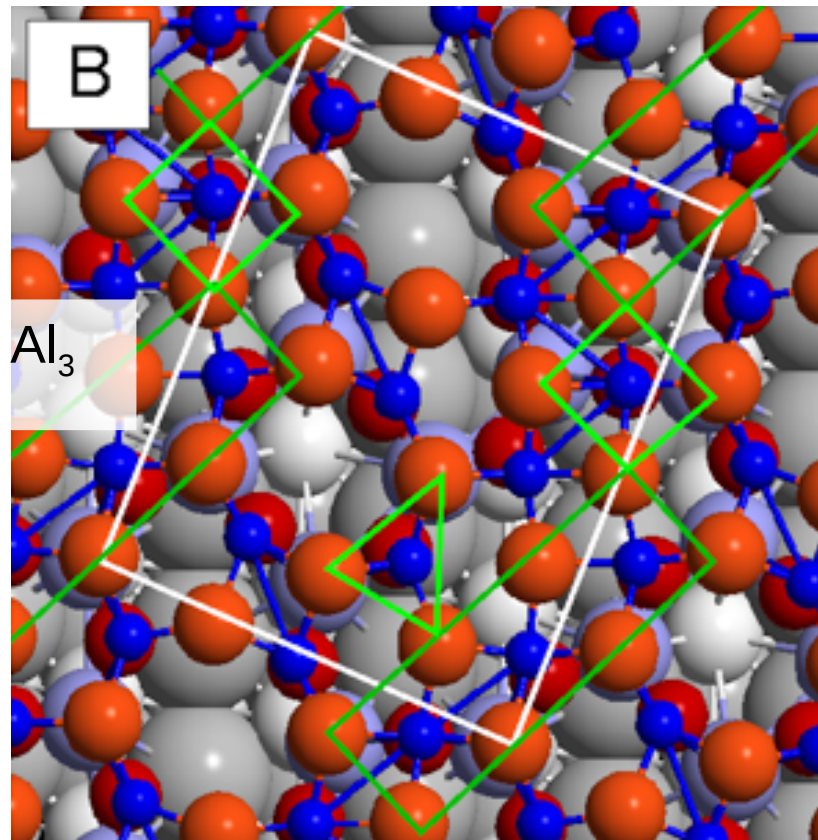
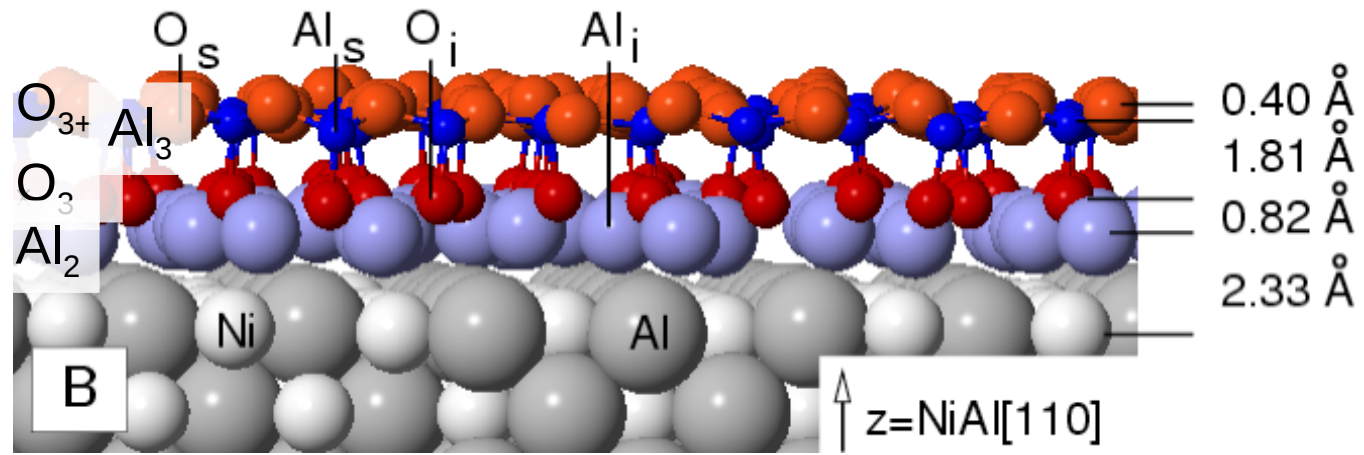
# Aluminium oxide on NiAl(110)



- Non-stoichiometric: not  $\text{Al}_2\text{O}_3$  but  $\text{Al}_{10}\text{O}_{13}$   
not  $(\text{NiAl})\text{-Al}_2\text{O}_3\text{Al}_2\text{O}_3$   
but  $(\text{NiAl})\text{-Al}_2\text{O}_3\text{Al}_3\text{O}_3$  (approximately)
- Remove Al atoms, molecular dynamics at finite temperature



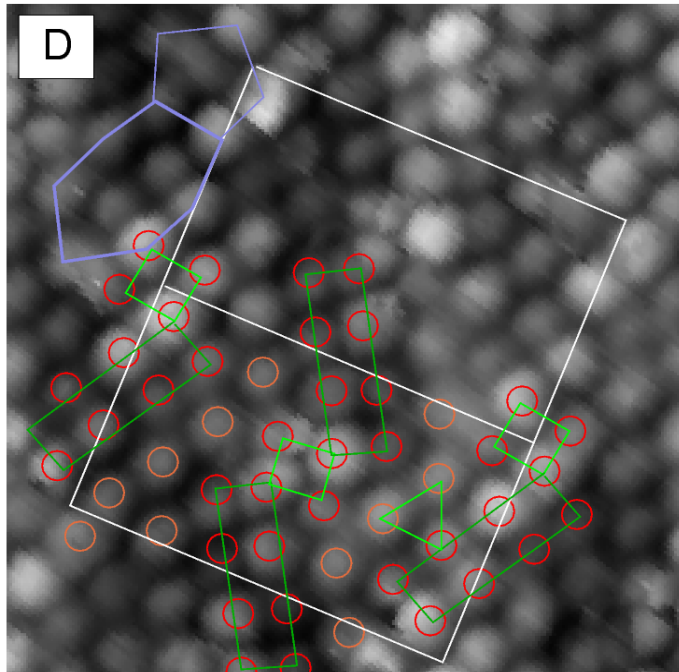
# STM



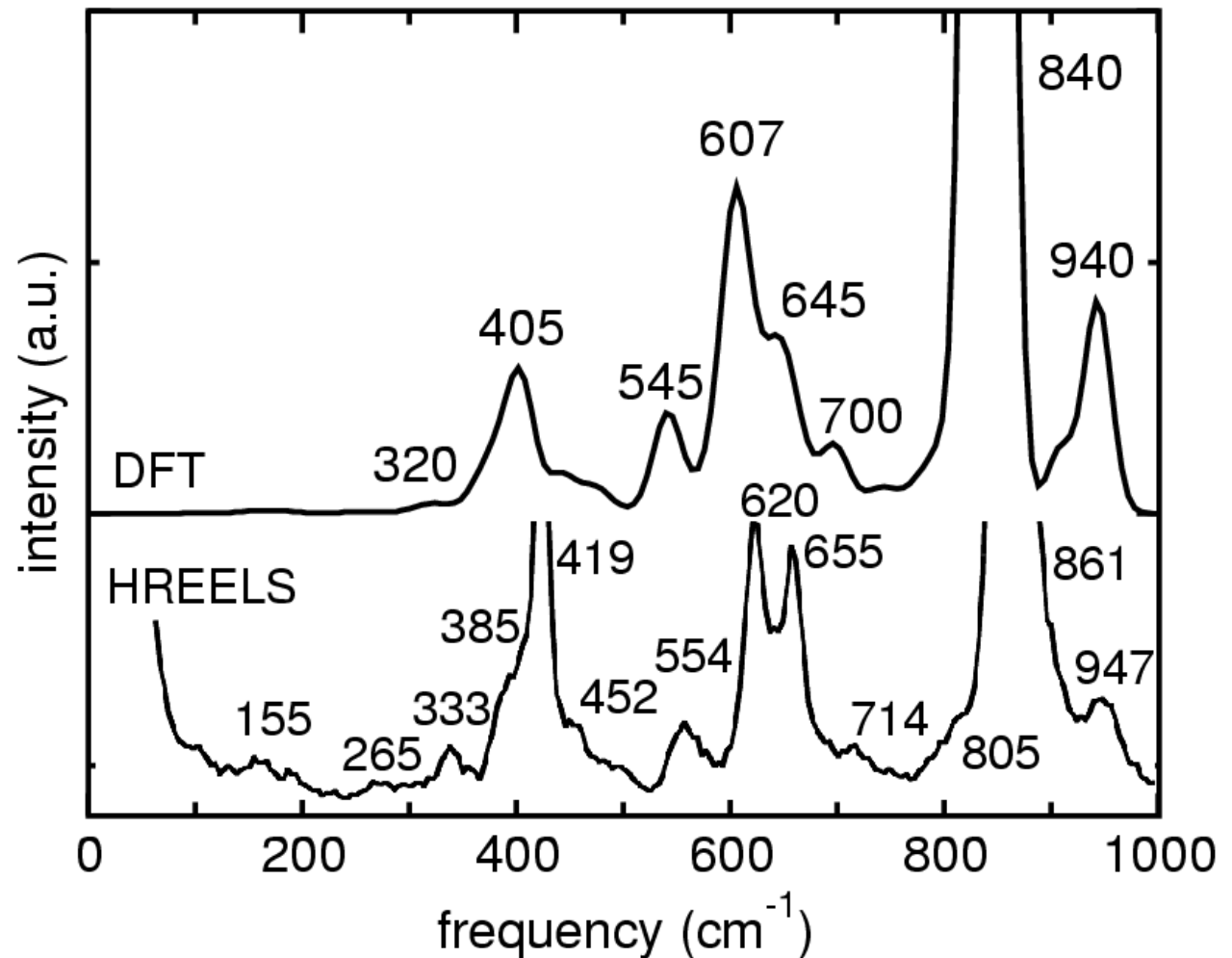
# HREELS

High Resolution Electron-Electron Loss Spectroscopy: measures the energy loss of incident electrons when inelastically scattered on matter (vibrational and electronic excitations).

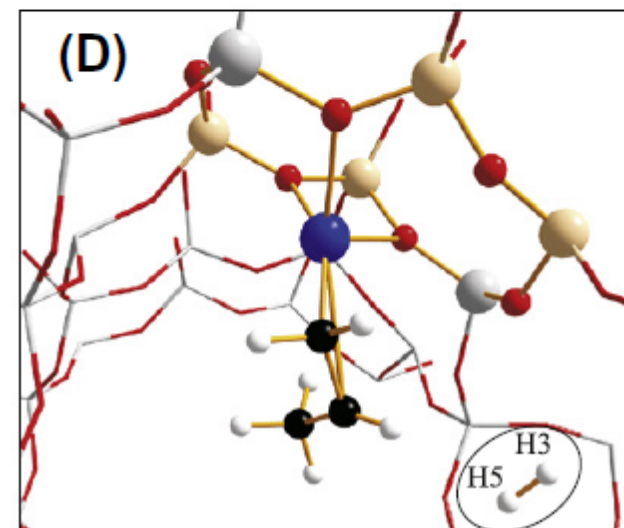
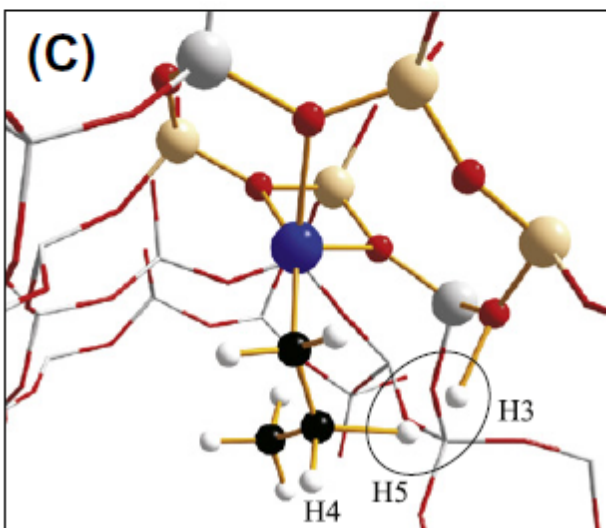
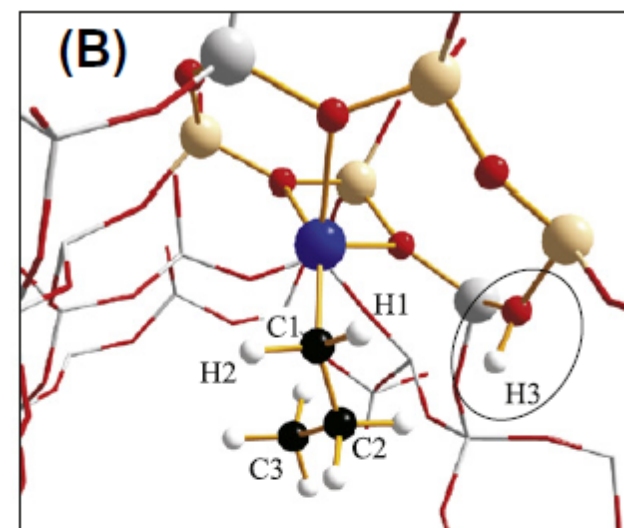
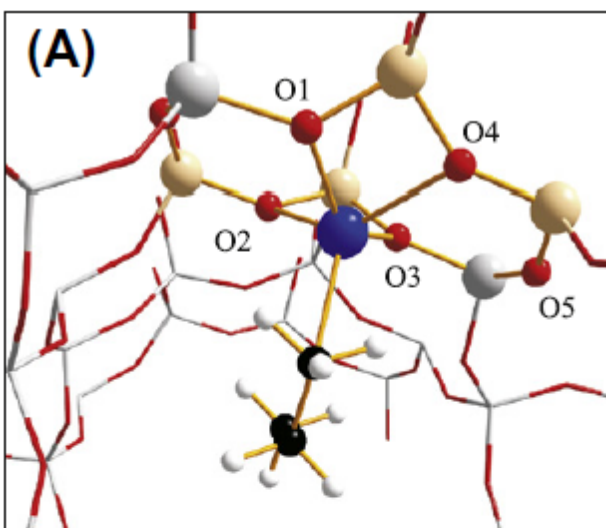
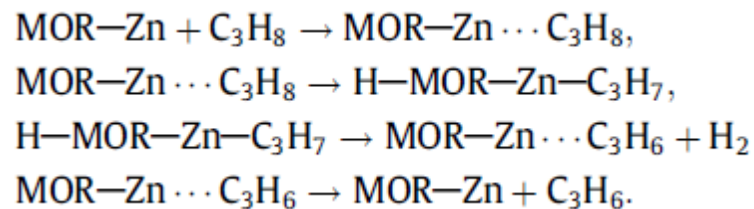
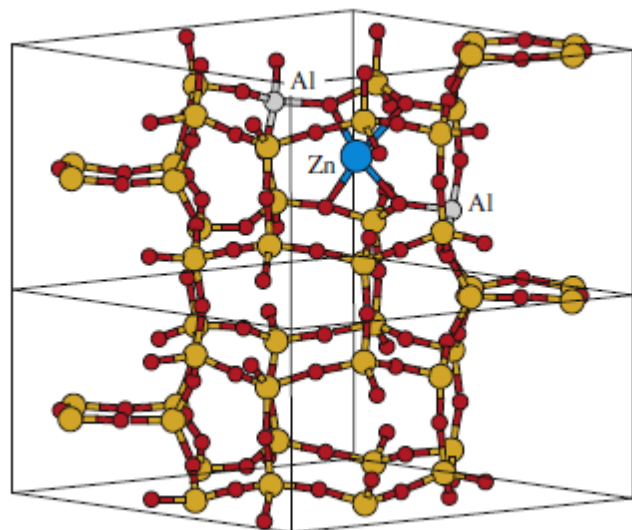
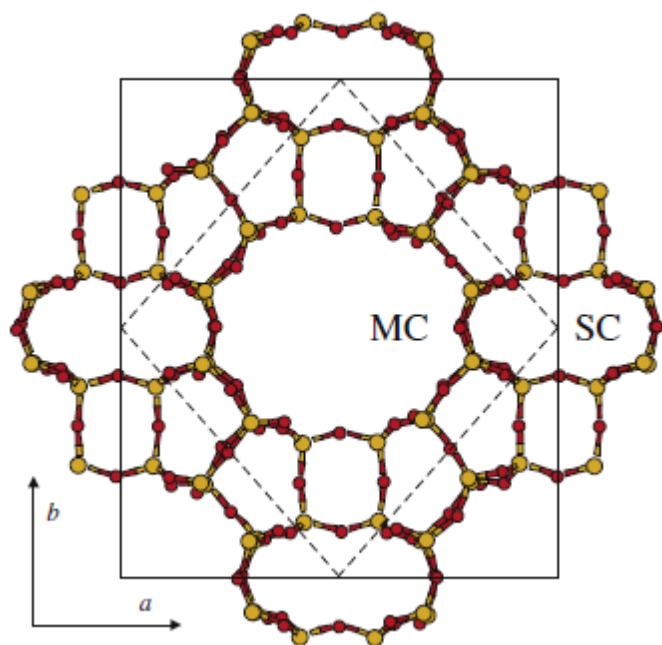
Exp: Frank *et al.*, Surf. Sci. 492, 270 (2001)

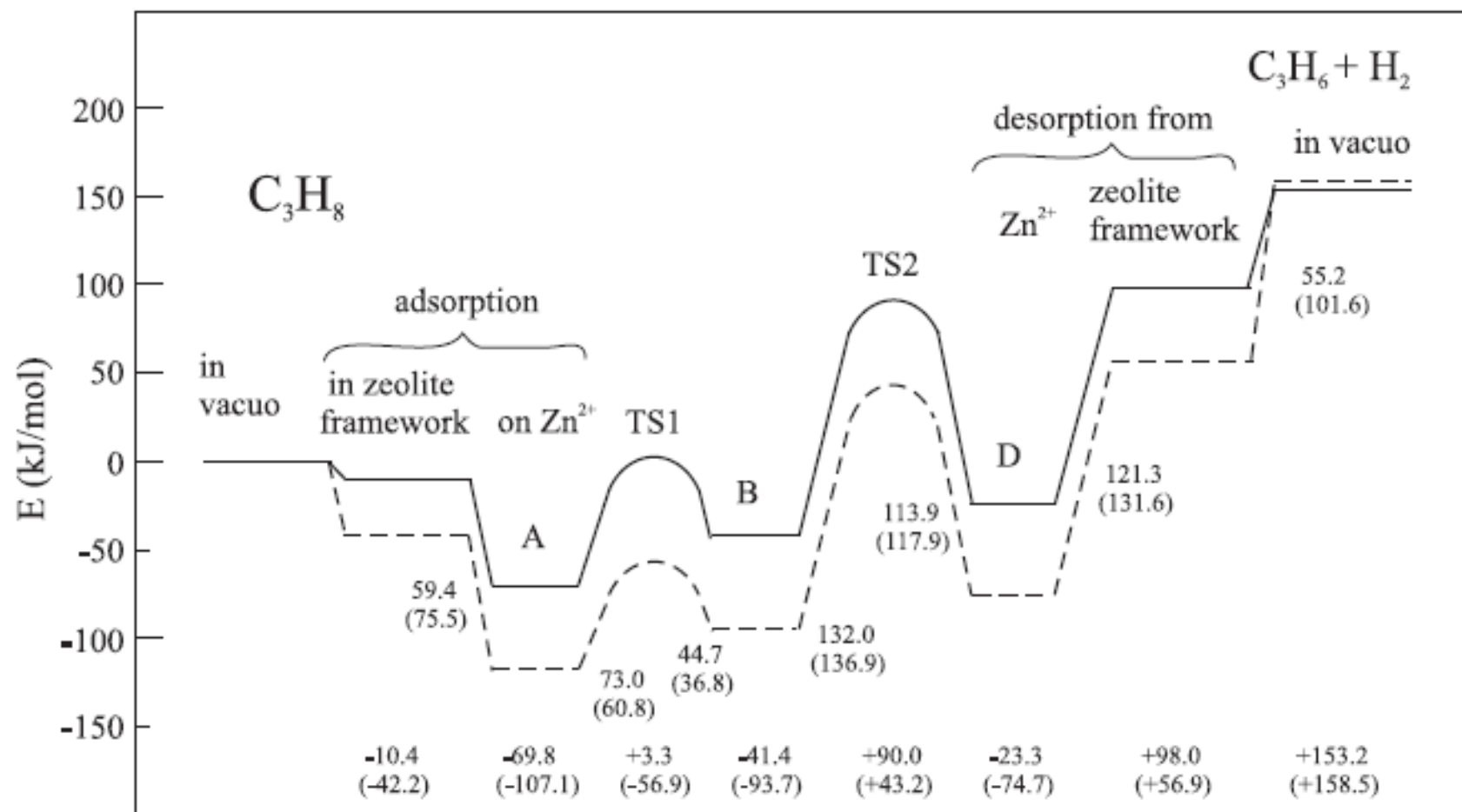
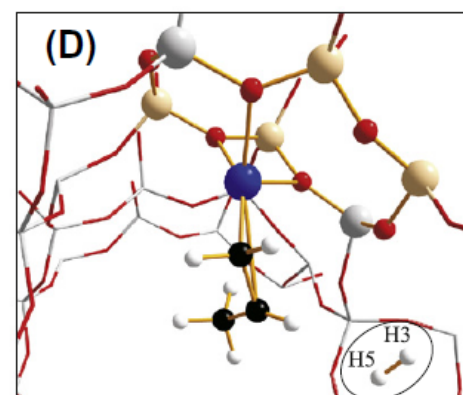
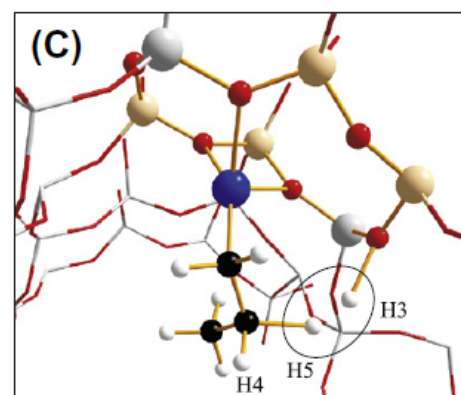
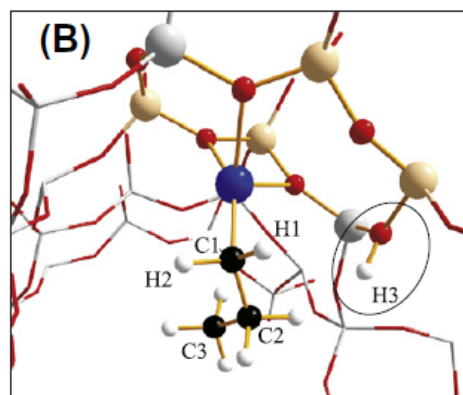
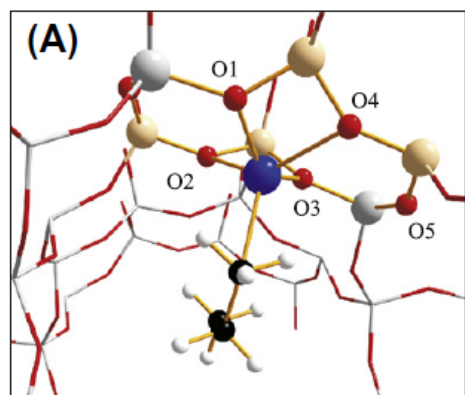


Kresse *et al.*,  
Science 308, 1440 (2005)



# Catalysis: dehydrogenation of propane in Mordenite





# Beyond DFT?

Lattice constants and Bulk moduli:  
AIP, AIAs, BAs, BP, Si, C, SiC, MgO, and LiF

	LDA		PBE		HF	
	$\Delta a_0$	$\Delta B_0$	$\Delta a_0$	$\Delta B_0$	$\Delta a_0$	$\Delta B_0$
MRE	-1.4	3.5	0.8	-7.2	0.4	8.2
MARE	1.4	7.9	0.8	7.2	0.7	8.2

Atomization energy

	LDA	PBE
MRE (%)	17.3	-1.9
MARE (%)	17.3	3.4
ME (eV)	0.76	0.14

(All in %)

(More) accurate treatment of electronic correlation needed for, e.g.:

Band gaps (optical properties)

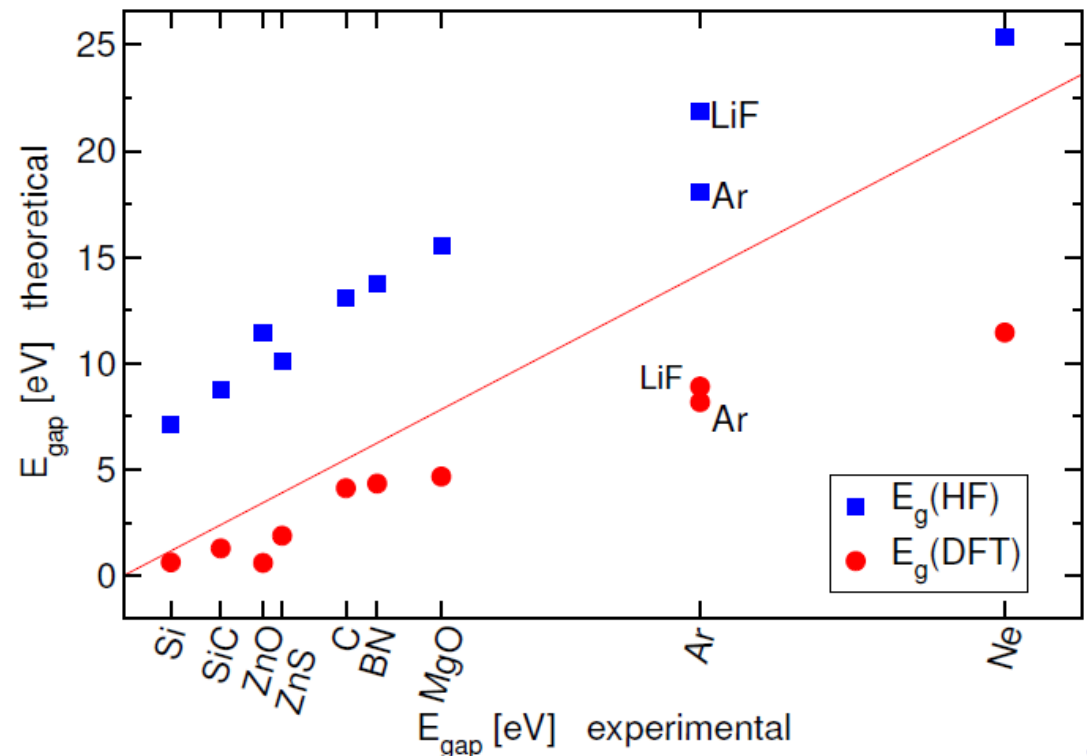
Total energy differences with chemical accuracy

(1 kcal/mol  $\approx$  40 meV):

atomization and formation energies  
reaction barriers

van der Waals interactions

Band gaps



# New Functionals

- New “density” functionals
  - GGA: AM05, PBEsol
  - meta-GGA: TPSS, revTPSS, M06-L
  - VdW-density functionals
- Hybrid functionals

# New density functionals (for solids)

AM05

PHYSICAL REVIEW B 72, 085108 (2005)

## Functional designed to include surface effects in self-consistent density functional theory

R. Armiento<sup>1,\*</sup> and A. E. Mattsson<sup>2,†</sup>

<sup>1</sup>*Department of Physics, Royal Institute of Technology, AlbaNova University Center, SE-106 91 Stockholm, Sweden*

<sup>2</sup>*Computational Materials and Molecular Biology MS 1110, Sandia National Laboratories, Albuquerque, New Mexico 87185-1110, USA*

PBEsol

PRL 100, 136406 (2008)

PHYSICAL REVIEW LETTERS

week ending  
4 APRIL 2008

## Restoring the Density-Gradient Expansion for Exchange in Solids and Surfaces

John P. Perdew,<sup>1</sup> Adrienn Ruzsinszky,<sup>1</sup> Gábor I. Csonka,<sup>2</sup> Oleg A. Vydrov,<sup>3</sup> Gustavo E. Scuseria,<sup>3</sup> Lucian A. Constantin,<sup>4</sup>  
Xiaolan Zhou,<sup>1</sup> and Kieron Burke<sup>5</sup>

<sup>1</sup>*Department of Physics and Quantum Theory Group, Tulane University, New Orleans, Louisiana 70118, USA*

<sup>2</sup>*Department of Chemistry, Budapest University of Technology and Economics, H-1521 Budapest, Hungary*

<sup>3</sup>*Department of Chemistry, Rice University, Houston, Texas 77005, USA*

<sup>4</sup>*Donostia International Physics Center, E-20018, Donostia, Basque Country*

<sup>5</sup>*Departments of Chemistry and of Physics, University of California, Irvine, Irvine, California 92697, USA*

Better description of lattice constants and bulk moduli, and (jellium) surface energies

TABLE I. Statistical data for the equilibrium lattice constants ( $\text{\AA}$ ) of the 18 test solids of Ref. 38 at 0 K calculated from the SJEOS. The Murnaghan EOS yields identical results within the reported number of decimal places. Experimental low temperature (5–50 K) lattice constants are from Ref. 56 (Li), Ref. 57 (Na, K), Ref. 58 (Al, Cu, Rh, Pd, Ag), and Ref. 59 (NaCl). The rest are based on room temperature values from Ref. 60 (C, Si, SiC, Ge, GaAs, NaF, LiF, MgO) and Ref. 57 (LiCl), corrected to the  $T=0$  limit using the thermal expansion from Ref. 58. An estimate of the zero-point anharmonic expansion has been subtracted out from the experimental values (cf. Table II). (The calculated values are precise to within 0.001  $\text{\AA}$  for the given basis sets, although GAUSSIAN GTO1 and GTO2 basis-set incompleteness limits the accuracy to 0.02  $\text{\AA}$ .) GTO1: the basis set used in Ref. 38. GTO2: For C, Si, SiC, Ge, GaAs, and MgO, the basis sets were taken from Ref. 41. For the rest of the solids, the GTO1 basis sets and effective core potentials from Ref. 38 were used. The best theoretical values are in boldface. The LDA, PBEsol, and PBE GTO2 results are from Ref. 14. The SOGGA GTO1 results are from Ref. 15.

	LDA	LDA	PBEsol	PBEsol	PBEsol	AM05	SOGGA	PBE	PBE	PBE	TPSS
	GTO2	VASP	GTO2	BAND	VASP	VASP	GTO1	GTO2	VASP	BAND	BAND
ME <sup>a</sup> ( $\text{\AA}$ )	-0.047	-0.055	0.022	<b>0.010</b>	<b>0.012</b>	0.029	<b>0.009</b>	0.075	0.066	0.063	0.048
MAE <sup>b</sup> ( $\text{\AA}$ )	0.050	0.050	0.030	<b>0.023</b>	<b>0.023</b>	0.036	<b>0.024</b>	0.076	0.069	0.067	0.052
MRE <sup>c</sup> (%)	-1.07	-1.29	0.45	<b>0.19</b>	<b>0.24</b>	0.58	<b>0.19</b>	1.62	1.42	1.35	0.99
MARE <sup>d</sup> (%)	1.10	1.15	0.67	<b>0.52</b>	<b>0.52</b>	0.80	<b>0.50</b>	1.65	1.48	1.45	1.10

# Meta-GGAs

	Lattice constant	
	MRE	MARE
LDA	-1.73	1.73
PBE	1.10	1.29
PBEsol	-0.24	0.73
AM05	0.19	0.75
TPSS	0.73	0.90
revTPSS	0.29	0.68

	Atomization energy (solids)	
	MRE	MARE
LDA	16.5	16.5
PBE	-3.68	4.23
PBEsol	5.97	6.52
TPSS	-1.99	4.70
revTPSS	1.22	5.73

	Atomization energy (AE6 mol.)	
	MRE	MARE
PBE	3.2	4.2
PBEsol	8.1	8.1
TPSS	1.3	2.4
revTPSS	1.3	2.8

(All in %)

$$E_{xc} = \int d\mathbf{r} \rho(\mathbf{r}) \epsilon_{xc}[\rho(\mathbf{r}), \nabla\rho(\mathbf{r}), \tau(\mathbf{r})]$$

$$\tau(\mathbf{r}) = \sum_i 1/2 |\nabla\psi_i(\mathbf{r})|^2$$

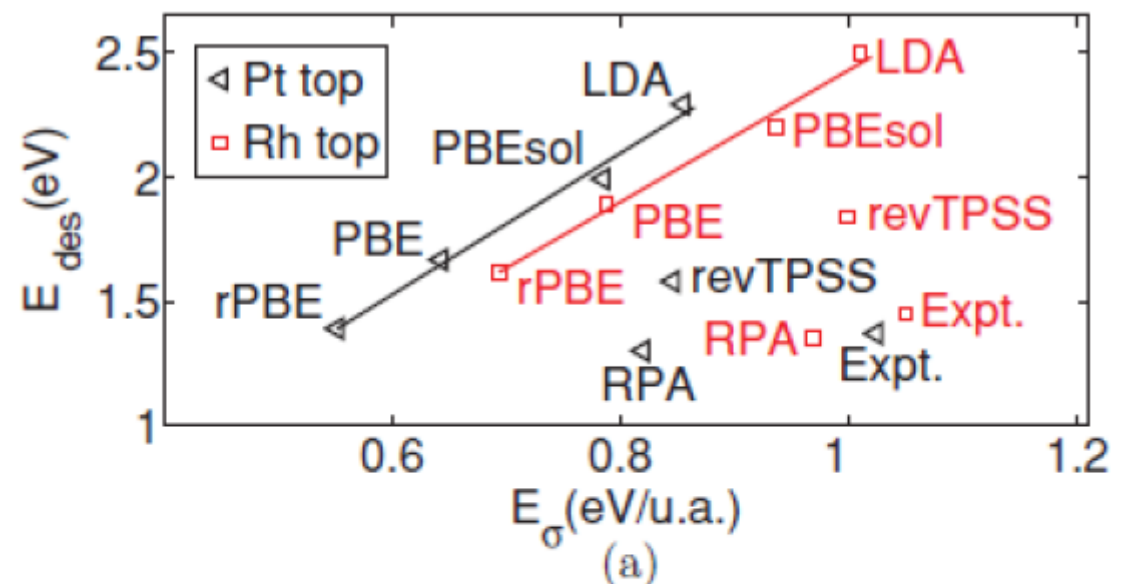
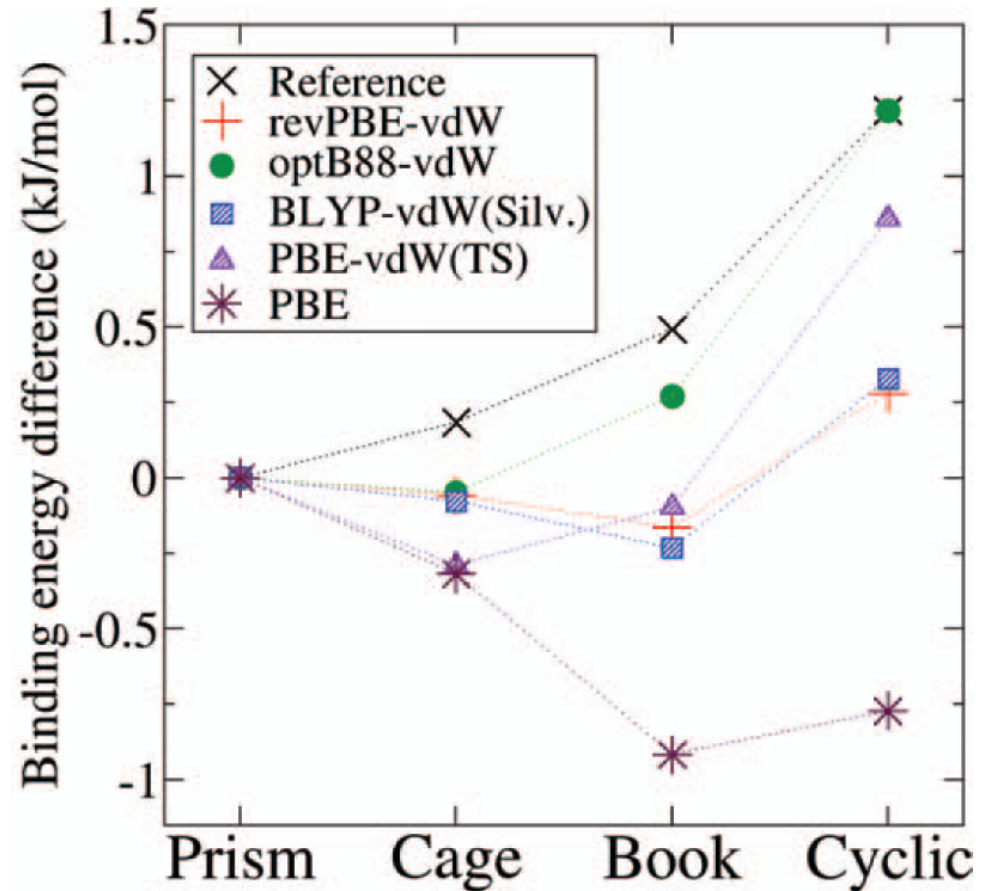
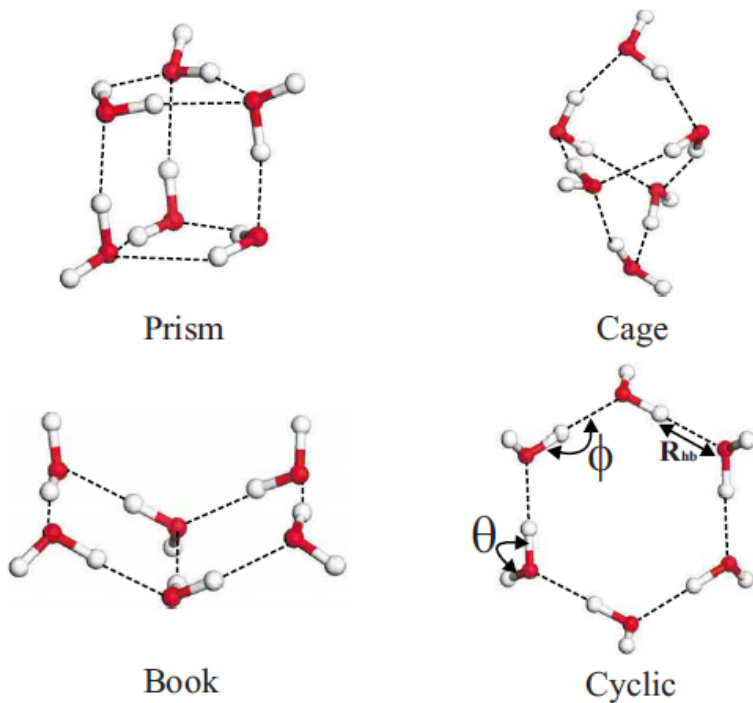


FIG. 1. (Color) (a) Atop CO desorption energy vs surface energies for Pt(111) and Rh(111). RPA values from Ref. 5, experimental surface energies from liquid-metal data (Refs. 23 and 24), and experimental CO desorption energies from Ref. 7. Surface energies are per surface-plane atom. (b) Exchange enhancement factors of

# Van der Waals - DFT

$$E_c^{\text{nl}} = \int \int \rho(\mathbf{r}) \phi(\mathbf{r}, \mathbf{r}') \rho(\mathbf{r}') d\mathbf{r} d\mathbf{r}'$$



# Hybrid functionals

Hartree-Fock-DFT hybrid:

$$E_{xc}^{\text{hyb.}} = aE_X^{\text{HF}} + (1 - a)E_X^{\text{DFT}} + E_c^{\text{DFT}}$$

where

$$E_x^{\text{HF}} \propto \sum_{\mathbf{k}n, \mathbf{q}m} \int \int d^3\mathbf{r} d^3\mathbf{r}' \frac{\psi_{\mathbf{k}n}^*(\mathbf{r})\psi_{\mathbf{q}m}(\mathbf{r})\psi_{\mathbf{q}m}^*(\mathbf{r}')\psi_{\mathbf{k}n}(\mathbf{r}')}{|\mathbf{r} - \mathbf{r}'|}$$

Solve a one-electron equation:

$$\left(-\frac{1}{2}\Delta + V_Z(\mathbf{r}) + V_H[n](\mathbf{r})\right)\psi_i(\mathbf{r}) + \int V_X(\mathbf{r}, \mathbf{r}')\psi_i(\mathbf{r}')d\mathbf{r}' = \epsilon_i\psi_i(\mathbf{r})$$

with an orbital dependent, non-local potential

(compare to DFT)

$$V_X(\mathbf{r}, \mathbf{r}') = -\sum_j^N \frac{\psi_j(\mathbf{r})\psi_j^*(\mathbf{r}')}{|\mathbf{r} - \mathbf{r}'|} \quad V_{xc}[n](\mathbf{r})\psi_i(\mathbf{r})$$

# How do they perform?

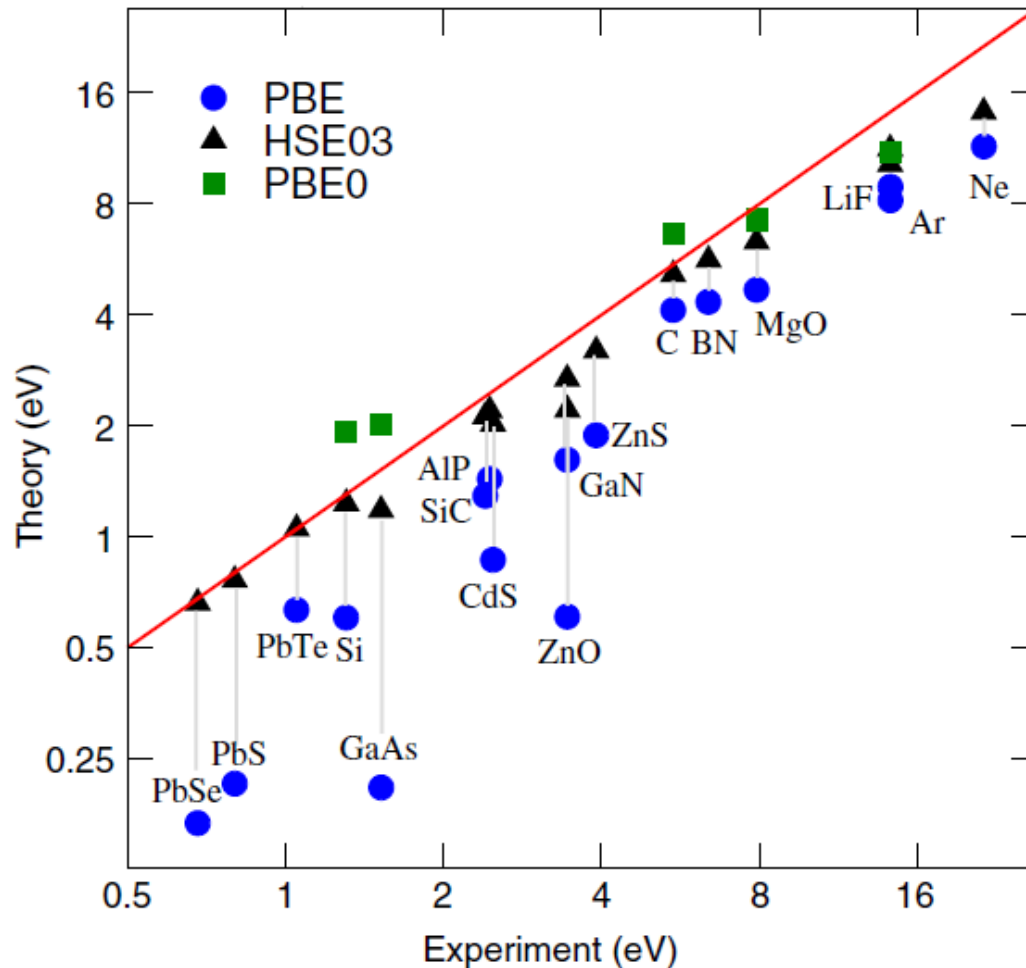


**Figure 8.** Band gaps from PBE, PBE0, and HSE03 calculations, plotted against data from experiment.

Lattice constant		
	MRE	MARE
PBE	0.8	1.0
PBE0	0.1	0.5
HSE	0.2	0.5
B3LYP	1.0	1.2

Bulk modulus		
	MRE	MARE
PBE	-9.8	9.4
PBE0	-1.2	5.7
HSE	-3.1	6.4
B3LYP	-10.2	11.4

Atomization energy		
	MRE	MARE
PBE	-1.9	3.4
PBE0	-6.5	7.4
HSE	-5.1	6.3
B3LYP	-17.6	17.6

(All in %)

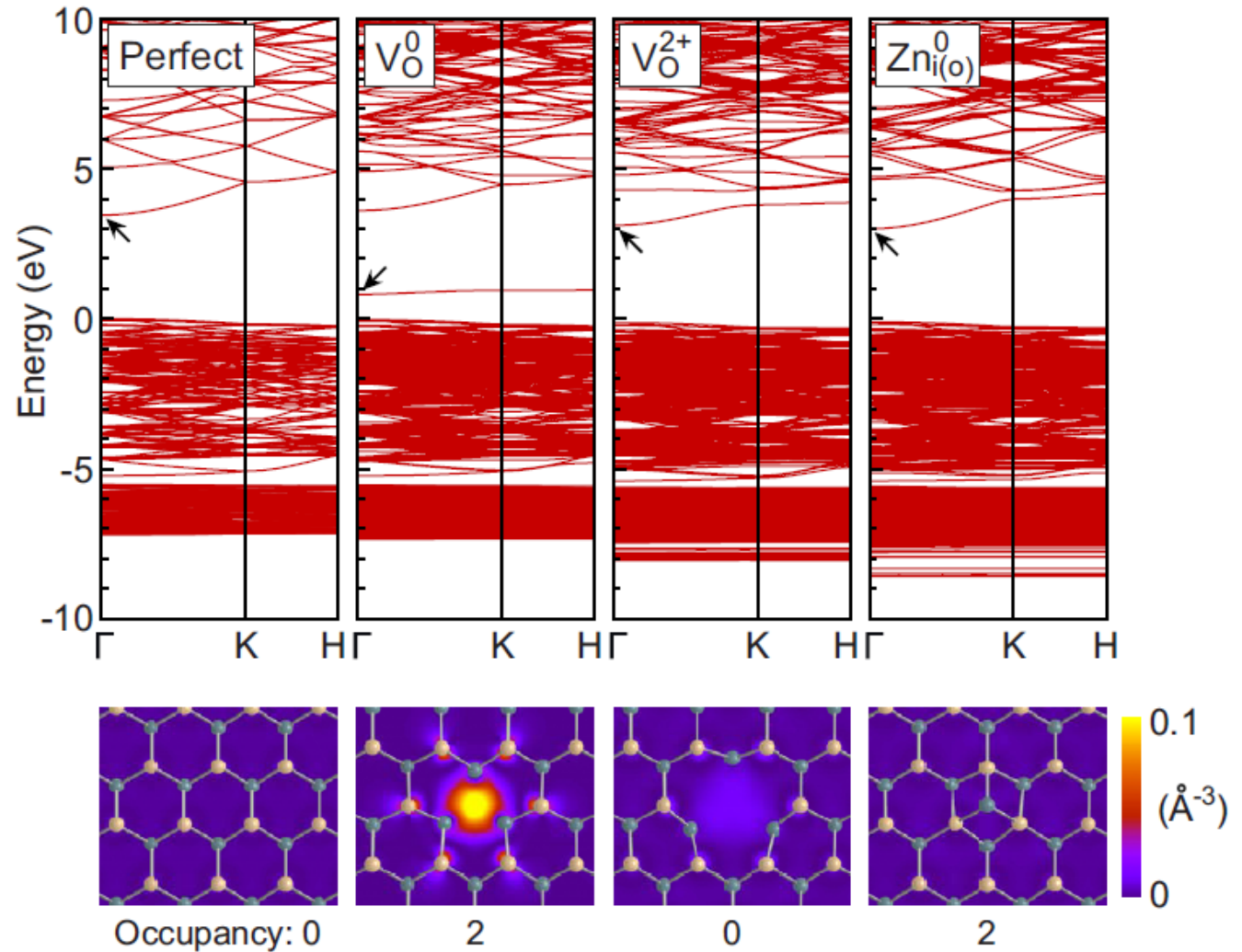
# Defects in ZnO

What is the source of n-type conductivity in ZnO?

- Oxygen vacancy:  
low formation energy  
deep trap
- Zinc interstitial:  
shallow donor  
high formation energy
- So?

Possibly: Hydrogen

Still not solved ...



# One-electron picture

DFT

$$\left( -\frac{1}{2}\Delta + V_{\text{ext}}(\mathbf{r}) + V_{\text{H}}(\mathbf{r}) + V_{\text{xc}}(\mathbf{r}) \right) \psi_{n\mathbf{k}}(\mathbf{r}) = \epsilon_{n\mathbf{k}} \psi_{n\mathbf{k}}(\mathbf{r})$$

HF-DFT Hybrids

$$\left( -\frac{1}{2}\Delta + V_{\text{ext}}(\mathbf{r}) + V_{\text{H}}(\mathbf{r}) \right) \psi_{n\mathbf{k}}(\mathbf{r}) + \int V_{\text{X}}(\mathbf{r}, \mathbf{r}') \psi_{n\mathbf{k}}(\mathbf{r}') d\mathbf{r}' = \epsilon_{n\mathbf{k}} \psi_{n\mathbf{k}}(\mathbf{r})$$

GW quasiparticles

$$\left( -\frac{1}{2}\Delta + V_{\text{ext}}(\mathbf{r}) + V_{\text{H}}(\mathbf{r}) \right) \psi_{n\mathbf{k}}(\mathbf{r}) + \int \Sigma(\mathbf{r}, \mathbf{r}', E_{n\mathbf{k}}) \psi_{n\mathbf{k}}(\mathbf{r}') d\mathbf{r}' = E_{n\mathbf{k}} \psi_{n\mathbf{k}}(\mathbf{r})$$

# GW

$$\left(-\frac{1}{2}\Delta + V_{\text{ext}}(\mathbf{r}) + V_{\text{H}}(\mathbf{r})\right) \psi_{n\mathbf{k}}(\mathbf{r}) + \int \Sigma(\mathbf{r}, \mathbf{r}', E_{n\mathbf{k}}) \psi_{n\mathbf{k}}(\mathbf{r}') d\mathbf{r}' = E_{n\mathbf{k}} \psi_{n\mathbf{k}}(\mathbf{r})$$

The “self-energy”:

$$\Sigma = iGW$$

The Green's function:

$$G(\mathbf{r}, \mathbf{r}', \omega) = \sum_n \frac{\psi_n(\mathbf{r}) \psi_n^*(\mathbf{r}')}{\omega - \epsilon_n + i\eta \operatorname{sgn}(\epsilon_n - \mu)}$$

Screened Coulomb int.

$$W = \epsilon^{-1} \nu$$

dielectric screening

$$\epsilon^{-1} = 1 + \nu\chi$$

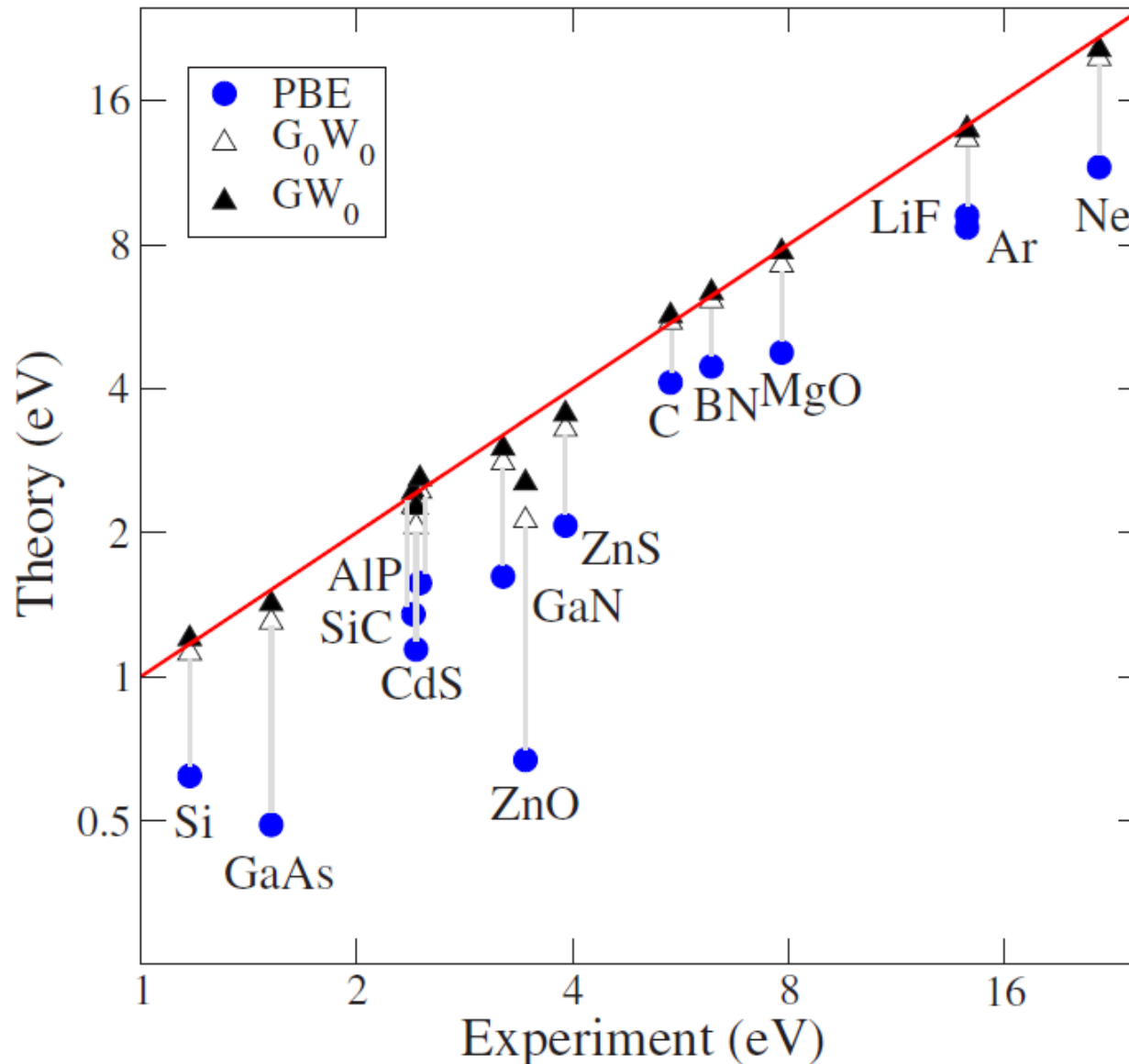
Random-Phase-Approx. (RPA)

$$\chi = \chi^0 + \chi^0 \nu \chi$$

IP polarizability (Adler&Wiser), the bottleneck (scales as  $N^4$ ):

$$\chi_{\mathbf{G}, \mathbf{G}'}^0(\mathbf{q}, \omega) = \frac{1}{\Omega} \sum_{nn'\mathbf{k}} 2w_{\mathbf{k}} (f_{n'\mathbf{k}+\mathbf{q}} - f_{n\mathbf{k}}) \times \frac{\langle \psi_{n'\mathbf{k}+\mathbf{q}} | e^{i(\mathbf{q}+\mathbf{G})\mathbf{r}} | \psi_{n\mathbf{k}} \rangle \langle \psi_{n\mathbf{k}} | e^{-i(\mathbf{q}+\mathbf{G}')\mathbf{r}'} | \psi_{n'\mathbf{k}+\mathbf{q}} \rangle}{\epsilon_{n'\mathbf{k}+\mathbf{q}} - \epsilon_{n\mathbf{k}} - \omega - i\eta}$$

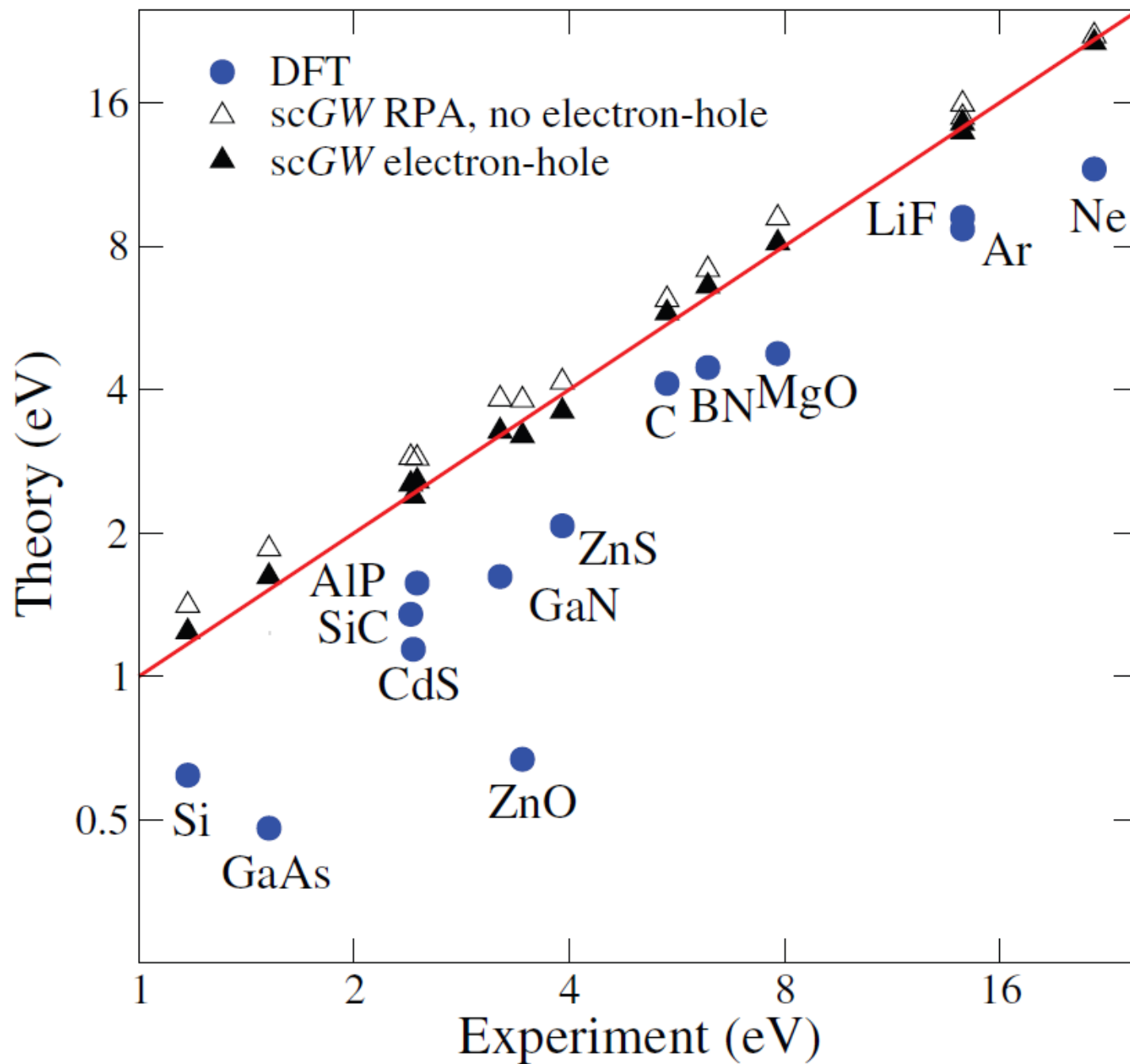
# G0W0(PBE) and GW0 QP-gaps



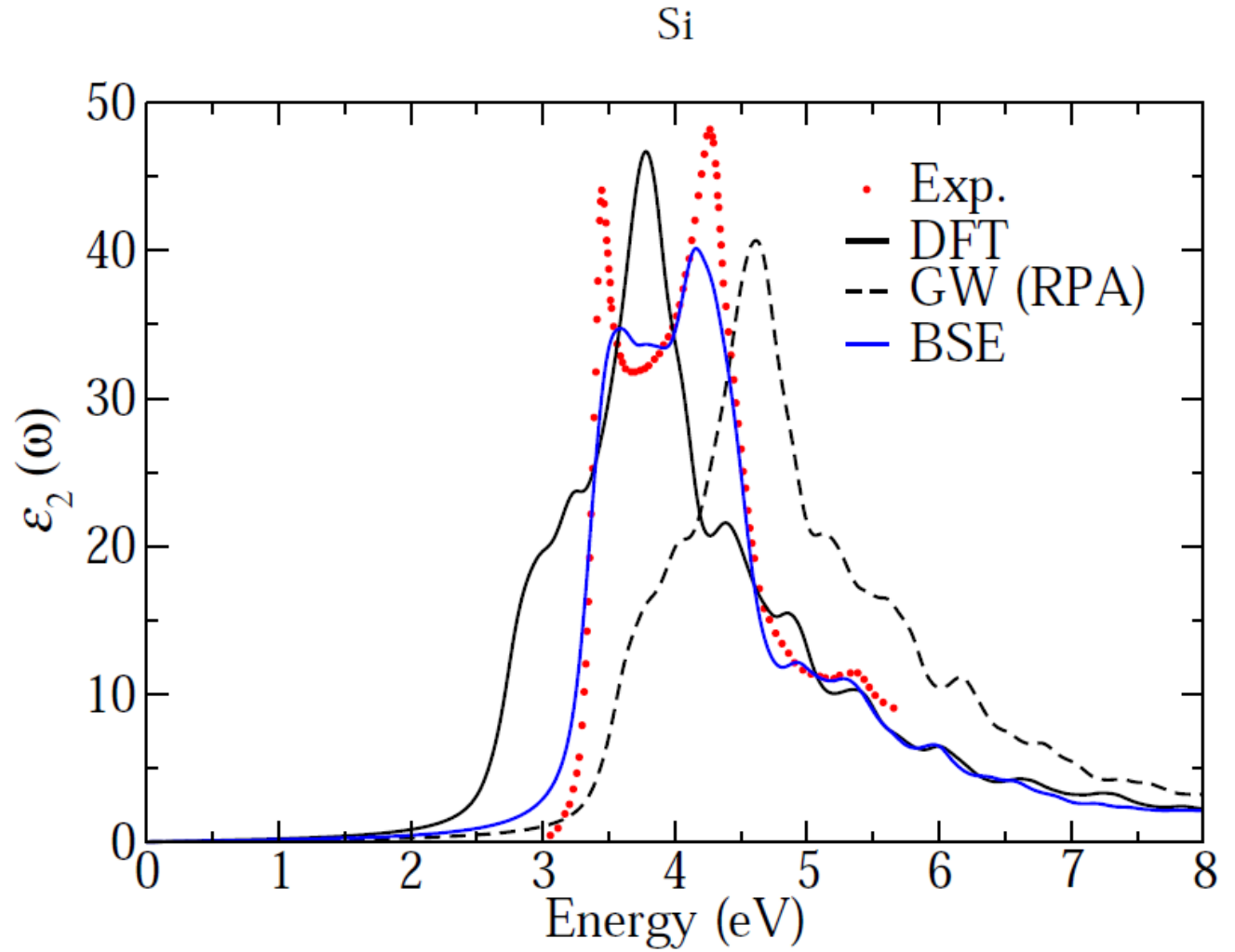
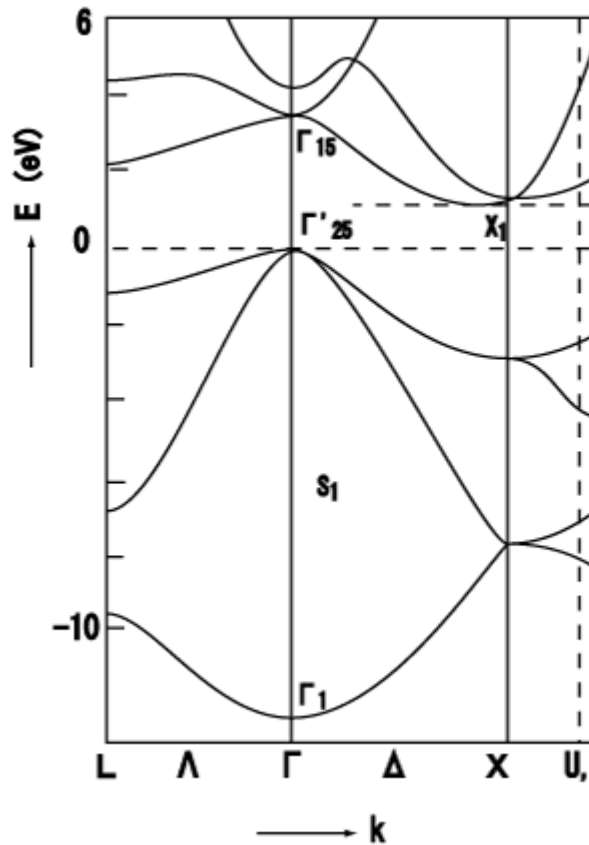
$G_0W_0$ : MARE=8.5% and  $GW_0$ : MARE=4.5%

# Fully self-consistent GW

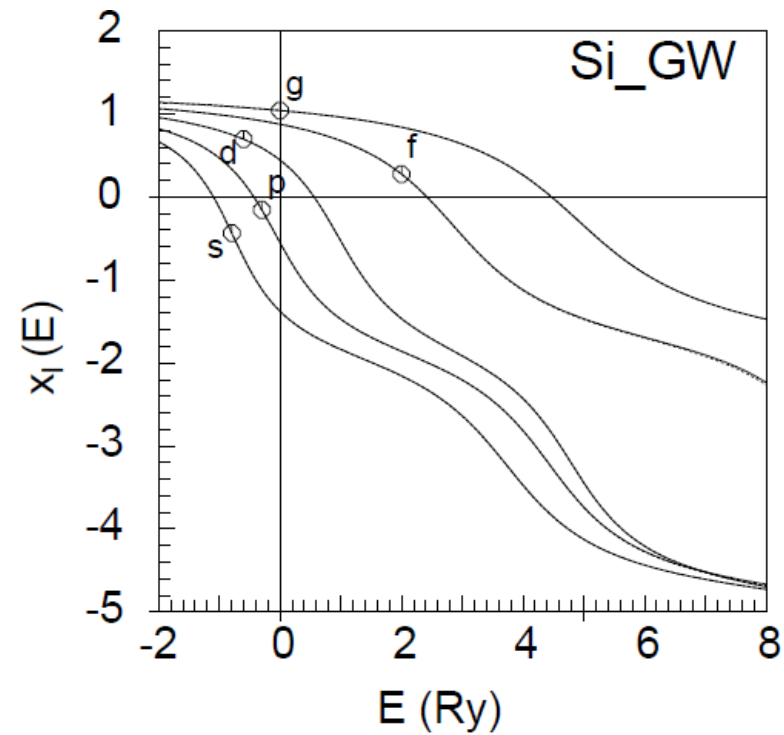
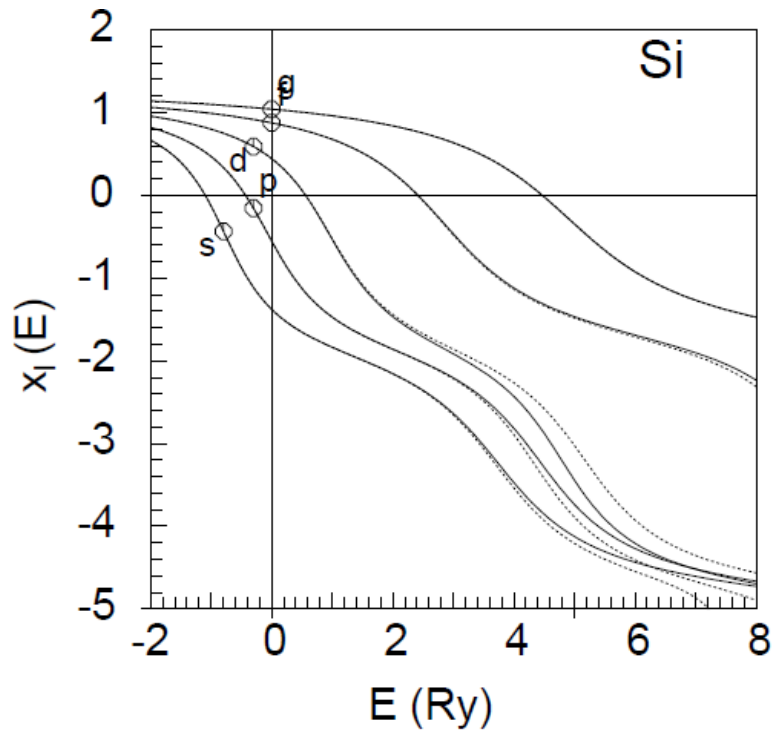
G. Kresse *et al.*, PRL 99, 246403 (2007)



# Bethe-Salpeter-Equation



# \*\_GW potentials



$\Delta(\text{PAW})_{(\text{VASP})} = 0.4 \text{ meV/atom}$

H																	He				
0,0																	0,0				
Li	Be															B	C	N	O	F	Ne
0,1	0,5															0,2	0,2	0,7	0,1	0,1	0,1
Na	Mg															Al	Si	P	S	Cl	Ar
0,4	0,0															0,3	0,1	0,0	0,2	0,0	0,1
K	Ca	Sc	Ti	V	Cr	Mn	Fe	Co	Ni	Cu	Zn	Ga	Ge	As	Se	Br	Kr				
0,1	0,4	0,3	0,3	0,1	0,8	0,1	0,1	0,2	0,8	0,5	0,6	0,8	0,7	0,8	0,4	0,2	0,1				
Rb	Sr	Y	Zr	Nb	Mo	Tc	Ru	Rh	Pd	Ag	Cd	In	Sn	Sb	Te	I	Xe				
0,1	0,2	0,5	0,4	0,2	0,9	0,1	0,2	0,3	0,4	0,3	2,5	0,2	0,2	0,5	0,9	0,9	0,1				
Cs	Ba	Lu	Hf	Ta	W	Re	Os	Ir	Pt	Au	Hg	Tl	Pb	Bi	Po	At	Rn				
0,1	0,3	3,5	1,7	0,8	1,2	0,9	0,5	0,8	0,3	0,1	1,0	0,2	0,1	0,5	0,6		0,0				

# RPA (ACFDT)

The “RPA” total energy is given by:

$$E[n] = T_{KS}[\{\psi_i\}] + E_H[n] + E_x[\{\psi_i\}] + E_{\text{ion-el}}[n] + E_c$$

with

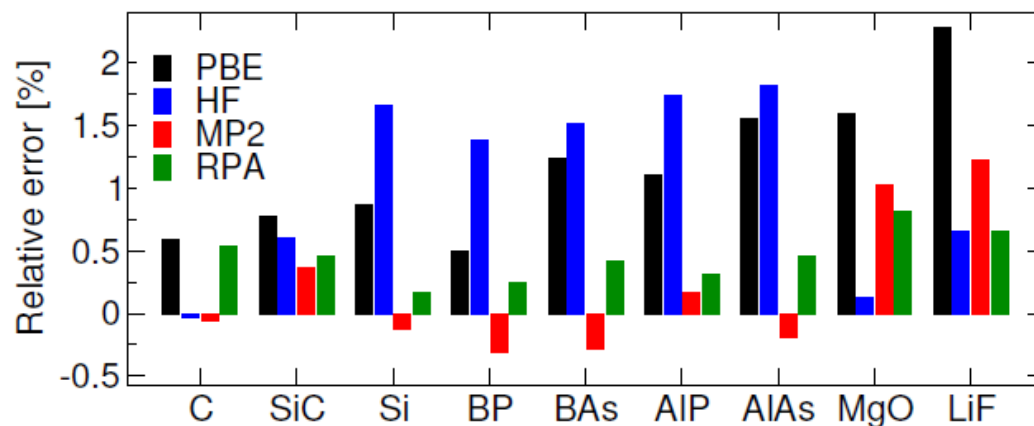
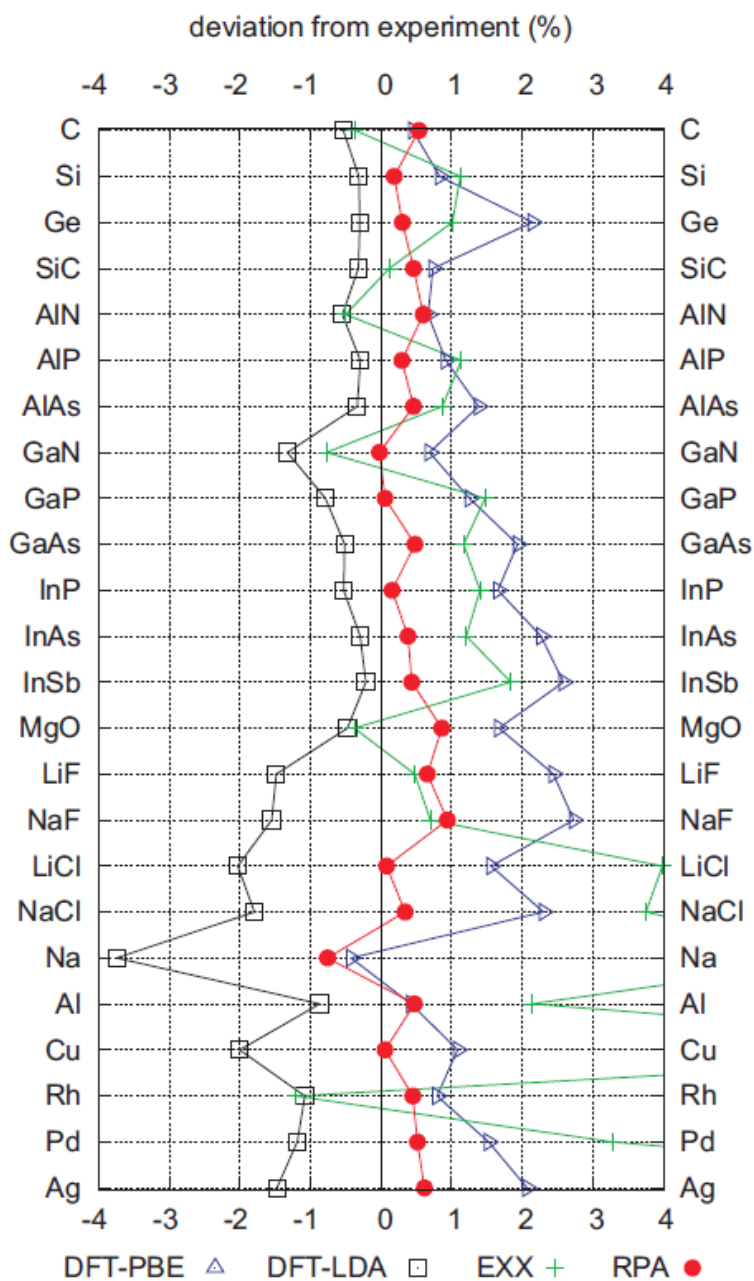
$$E_c = \int_0^\infty \frac{d\omega}{2\pi} \text{Tr}\{\ln[1 - \chi^0(i\omega)\nu] + \chi^0(i\omega)\nu\}$$

The main effort is again computing the IP-polarizability:

$$\chi_{\mathbf{G}\mathbf{G}'}^0(\mathbf{q}, i\omega) = \frac{1}{V} \sum_{n, n', \mathbf{k}} 2g_{\mathbf{k}}(f_{n'\mathbf{k}+\mathbf{q}} - f_{n\mathbf{k}}) \\ \times \frac{\langle \psi_{n'\mathbf{k}+\mathbf{q}} | e^{i(\mathbf{q}+\mathbf{G})\mathbf{r}} | \psi_{n\mathbf{k}} \rangle \langle \psi_{n\mathbf{k}} | e^{-i(\mathbf{q}+\mathbf{G}')\mathbf{r}} | \psi_{n'\mathbf{k}+\mathbf{q}} \rangle}{\epsilon_{n'\mathbf{k}+\mathbf{q}} - \epsilon_{n\mathbf{k}} - i\omega}$$

# RPA: lattice constants

J. Harl *et al.*, PRB 81, 115126 (2010)

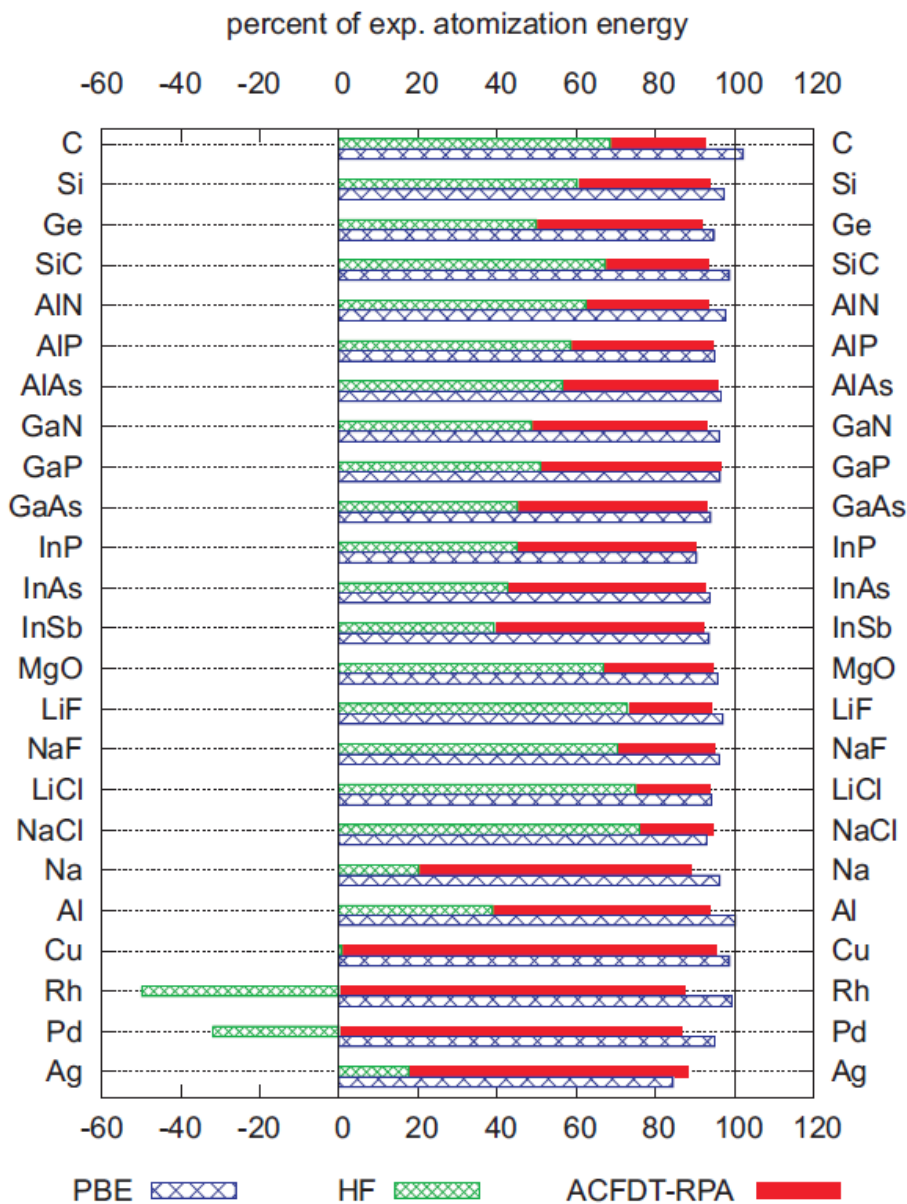


Deviations w.r.t. experiment  
(corrected for zero-point vibrations)

	MRE	MARE
PBE	1.2	1.2
HF	1.1	1.1
MP2	0.2	0.4
RPA	0.5	0.4

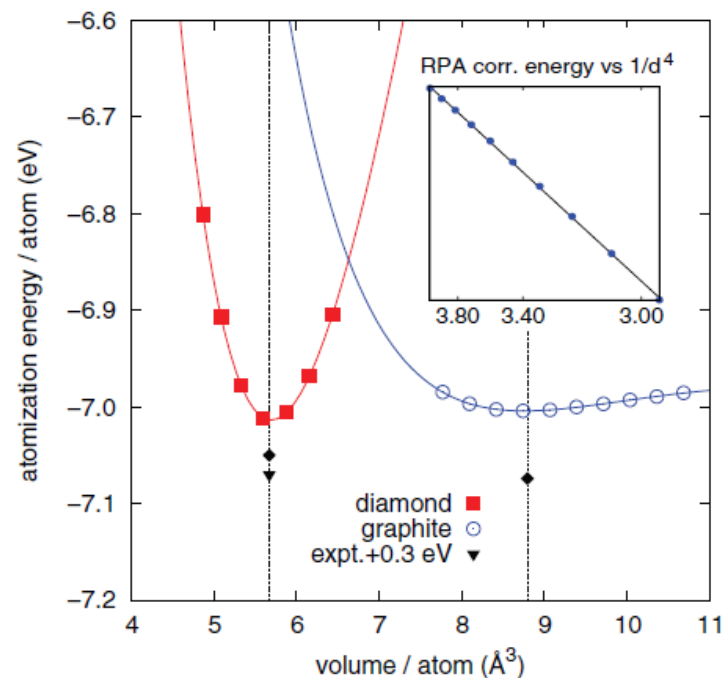
(in %)

# RPA: atomization energies



Harl *et al.* Phys. Rev. B **81**, 115126 (2010).

Harl *et al.* Phys. Rev. Lett. **103**, 056401 (2009).



	Atomization energies	
	MAE (eV)	MARE (%)
HF	1.65	
MP2	0.27	
PBE	0.17	5
LDA	0.74	18
RPA	0.30	7

# RPA: heats of formation

TABLE I. Heats of formation at  $T = 0$  K in kJ/mol (per formula unit) with respect to the elemental phases in their normal state under ambient conditions. Experimental values are collected in Ref. [33], if not otherwise stated, and have been corrected for zero-point vibrations (ZPV) (experimental values without corrections are in parentheses). The ZPV have been evaluated using harmonic *ab initio* phonon calculations.

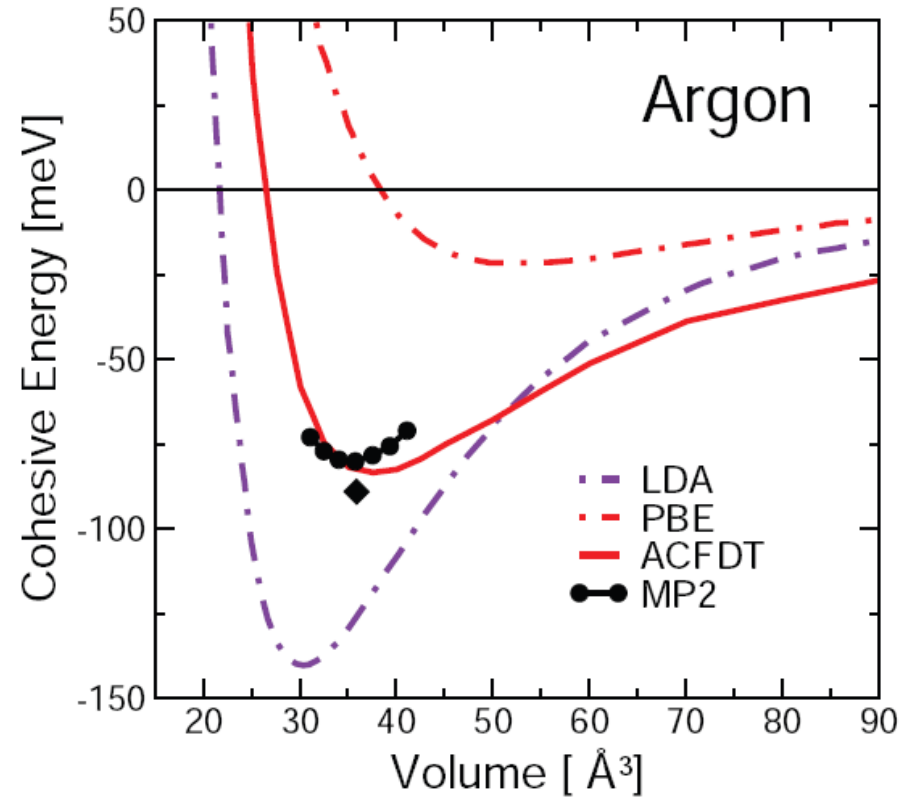
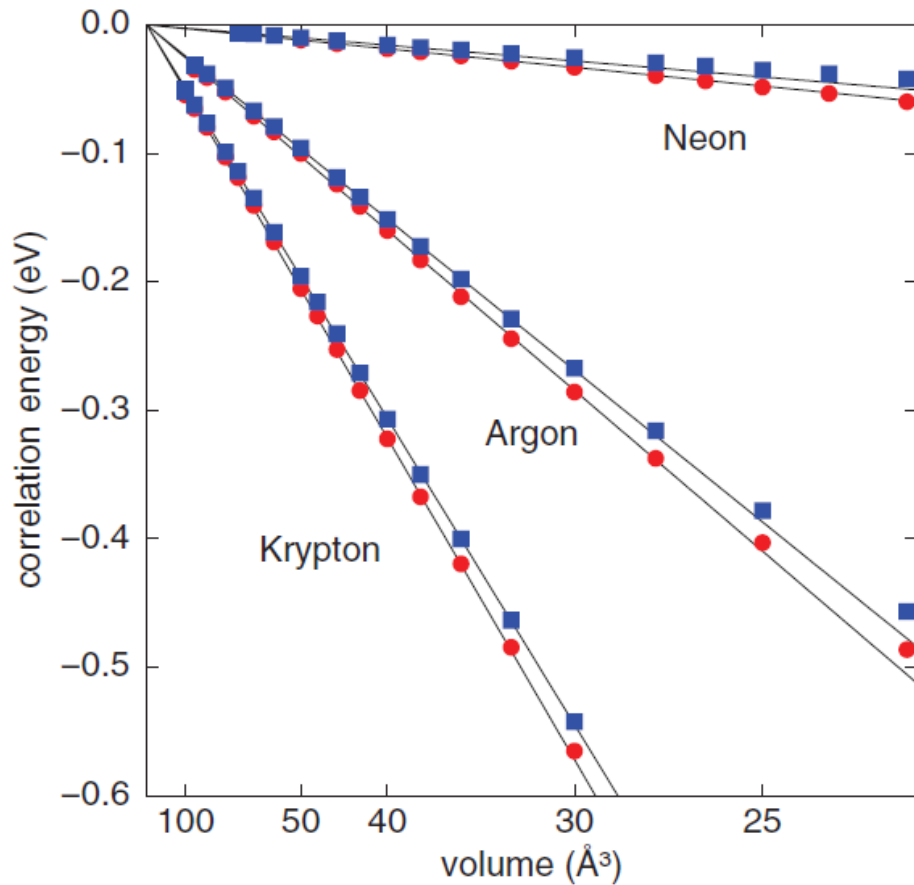
Solid	PBE	LDA	EXX	RPA	Expt.
LiF <sup>a</sup>	570	613	664	609	619 (614)
NaF	522	558	607	567	577 (573)
NaCl	355	381	433	405	413 (411)
MgO <sup>a</sup>	516	595	587	577	604 (597)
MgH <sub>2</sub> <sup>a</sup>	52	89	113	72	78 (68)
AlN	262	327	350	291	321 (313 <sup>b</sup> )
SiC	51	54	69	64	69 (72)

<sup>a</sup>bcc Li, hcp Mg, and rutile MgH<sub>2</sub> were considered in their experimental geometries, whereas for the other materials the theoretical minimum energy geometries were used.

<sup>b</sup>Ref. [34].

# RPA: noble gas solids

J. Harl and G. Kresse, PRB 77, 045136 (2008)



$C_6$  coefficients for noble gas solids

	RPA(LDA)	RPA(PBE)	Exp.
Ne	62	53	47
Ar	512	484	455
Kr	1030	980	895

# RPA: CO @ Pt(111) and Rh(111)

Too small surface energies and too large adsorption energies!

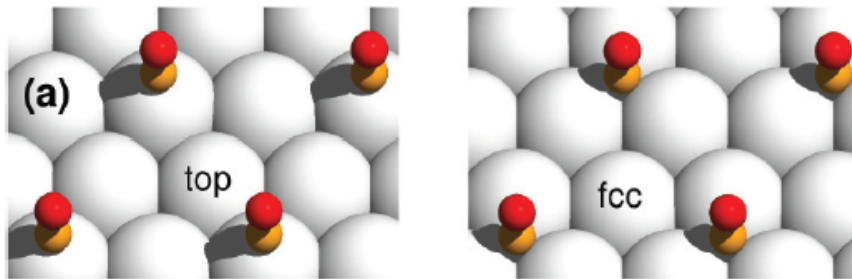
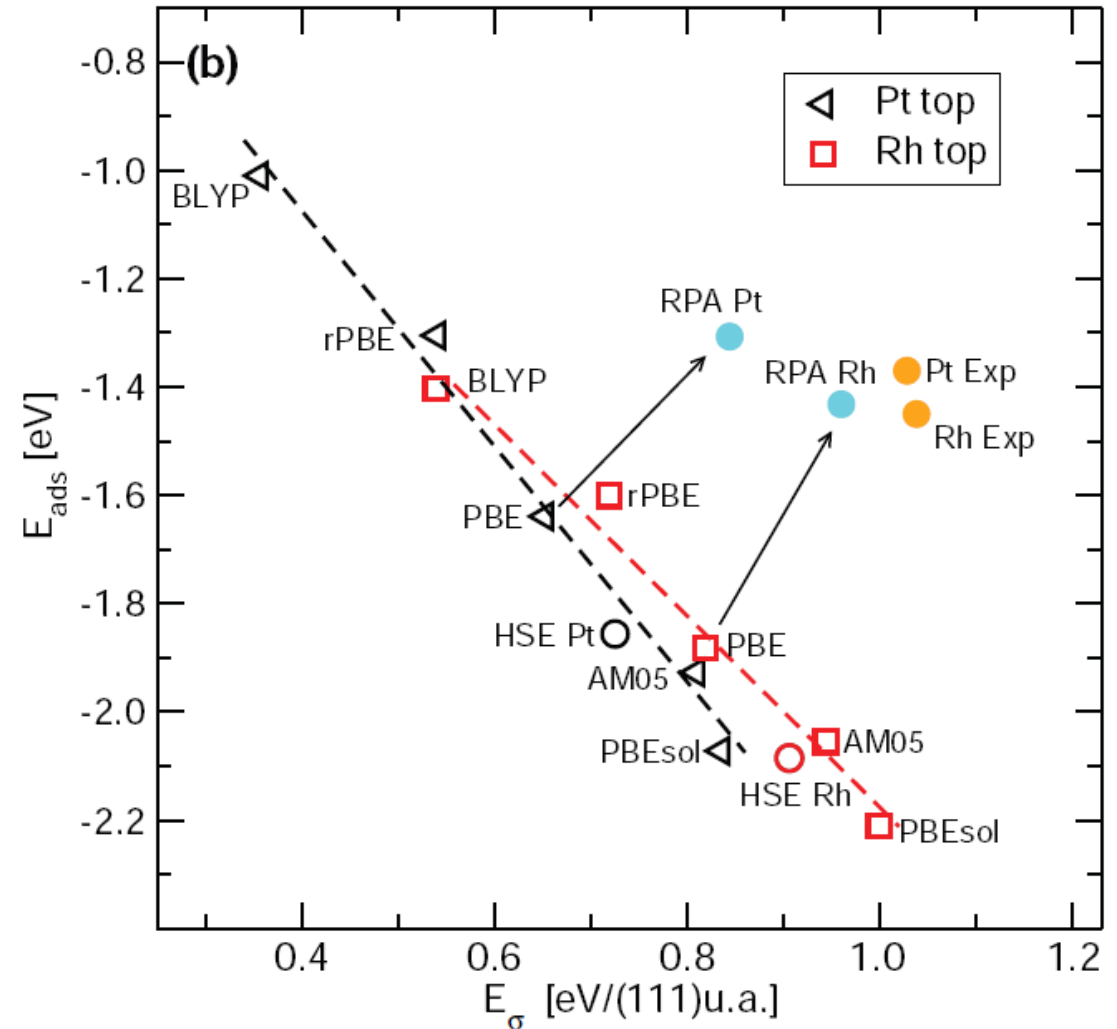


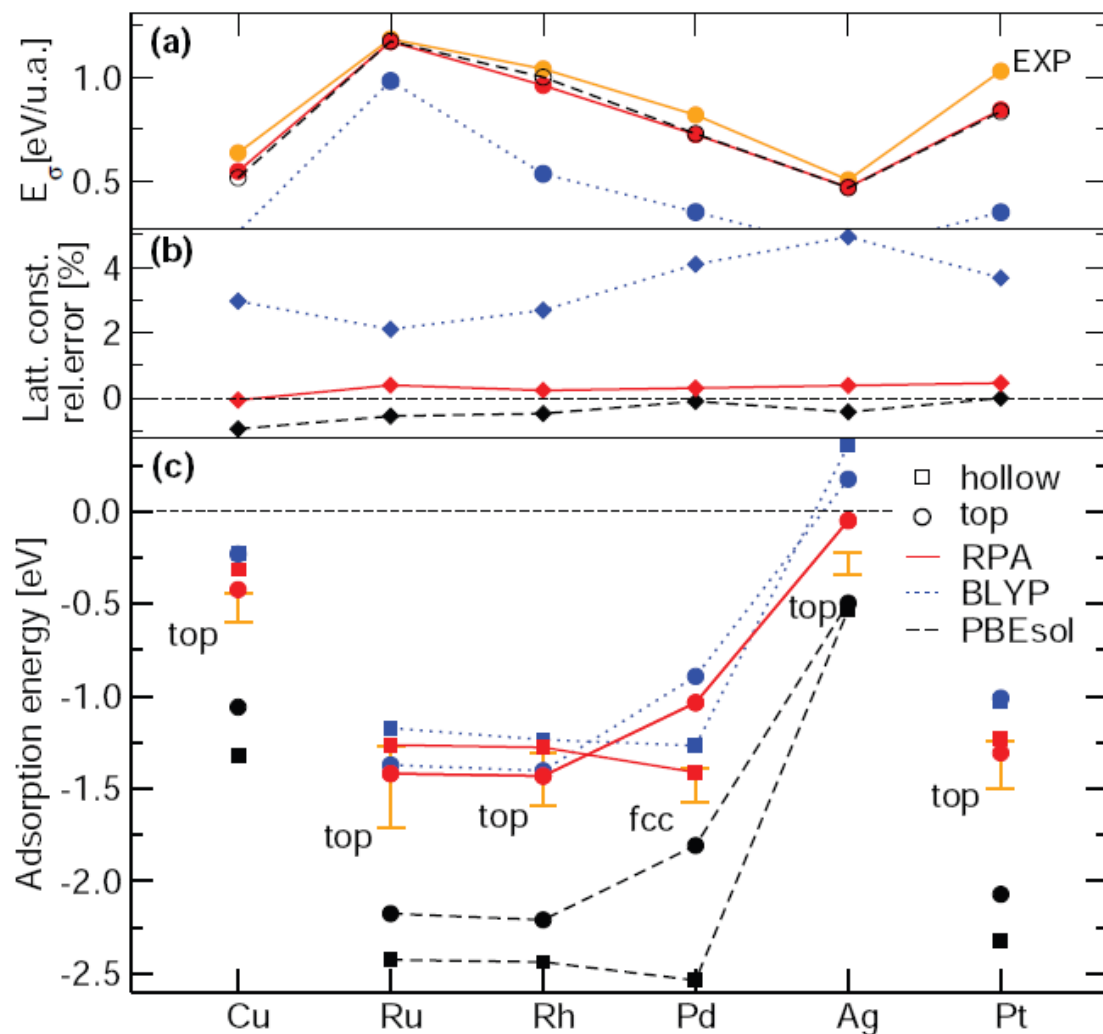
FIG. 1: Atop CO adsorption and surface energies for Pt(111) and Rh(111). (a) Considered CO adsorption geometries for a  $(2 \times 2)$  surface cell. Semi-local functionals predict CO to adsorb in the fcc hollow site coordinated to three metal atoms on Pt and Rh, whereas experiments unequivocally show adsorption atop a metal atom. (b) Atop adsorption energies versus surface energies for Pt(111) and Rh(111). Various semi-local functionals were used: AM05<sup>10</sup>, PBEsol<sup>11</sup>, PBE<sup>8</sup>, rPBE<sup>12</sup> and BLYP<sup>13</sup>, in order of increasing gradient corrections. Furthermore the hybrid functional HSE<sup>18</sup> based on the PBE functional was used.



Schimka *et al.* Nature Materials **9**, 741 (2010).

FIG. 3: Surface energies, lattice constants and adsorption energies. (a) Surface energies ( $E_\sigma$ ) for PBEsol, BLYP and RPA. Experimental data are from Ref. 24. (b) Lattice constants for PBEsol, RPA and BLYP. (c) Adsorption energies for the atop and hollow sites on Cu, late 4d metals and Pt for PBEsol and RPA and BLYP. Experimental data with error bars are from Ref. 25.

RPA:  
 Right site preference  
 Good adsorption energies  
 Excellent lattice constants  
 Good surface energies



Schimka *et al.* Nature Materials **9**, 741 (2010).

# Cubic-scaling RPA

M. Kaltak, J. Klimes, and G. Kresse, PRB 90, 054115 (2014)

Evaluate the Green's function in “imaginary” time:

$$G(\mathbf{r}, \mathbf{r}', i\tau) = \sum_n \psi_n(\mathbf{r}) \psi_n^*(\mathbf{r}') e^{-\epsilon_n \tau}$$

and the polarizability as:

$$\chi^0(\mathbf{r}, \mathbf{r}', i\tau) = -G(\mathbf{r}, \mathbf{r}', i\tau) G(\mathbf{r}', \mathbf{r}, -i\tau)$$

Followed by a cosine-transform:

$$\chi^0(\mathbf{r}, \mathbf{r}', i\tau) \xrightarrow{CT} \chi^0(\mathbf{r}, \mathbf{r}', i\omega)$$

Now the worst scaling step is

$$E_c = \int_0^\infty \frac{d\omega}{2\pi} \text{Tr}\{\ln[1 - \chi^0(i\omega)\nu] + \chi^0(i\omega)\nu\}$$

which scales as  $N^3$  due to the diagonalization involved in evaluating the “ln”

**But storing  $G$  and  $\chi$  is expensive!** → we need small sets of cleverly chosen “ $\tau$ ” and “ $\omega$ ”

[see Kaltak et al., JCTC 10, 2498 (2014)]

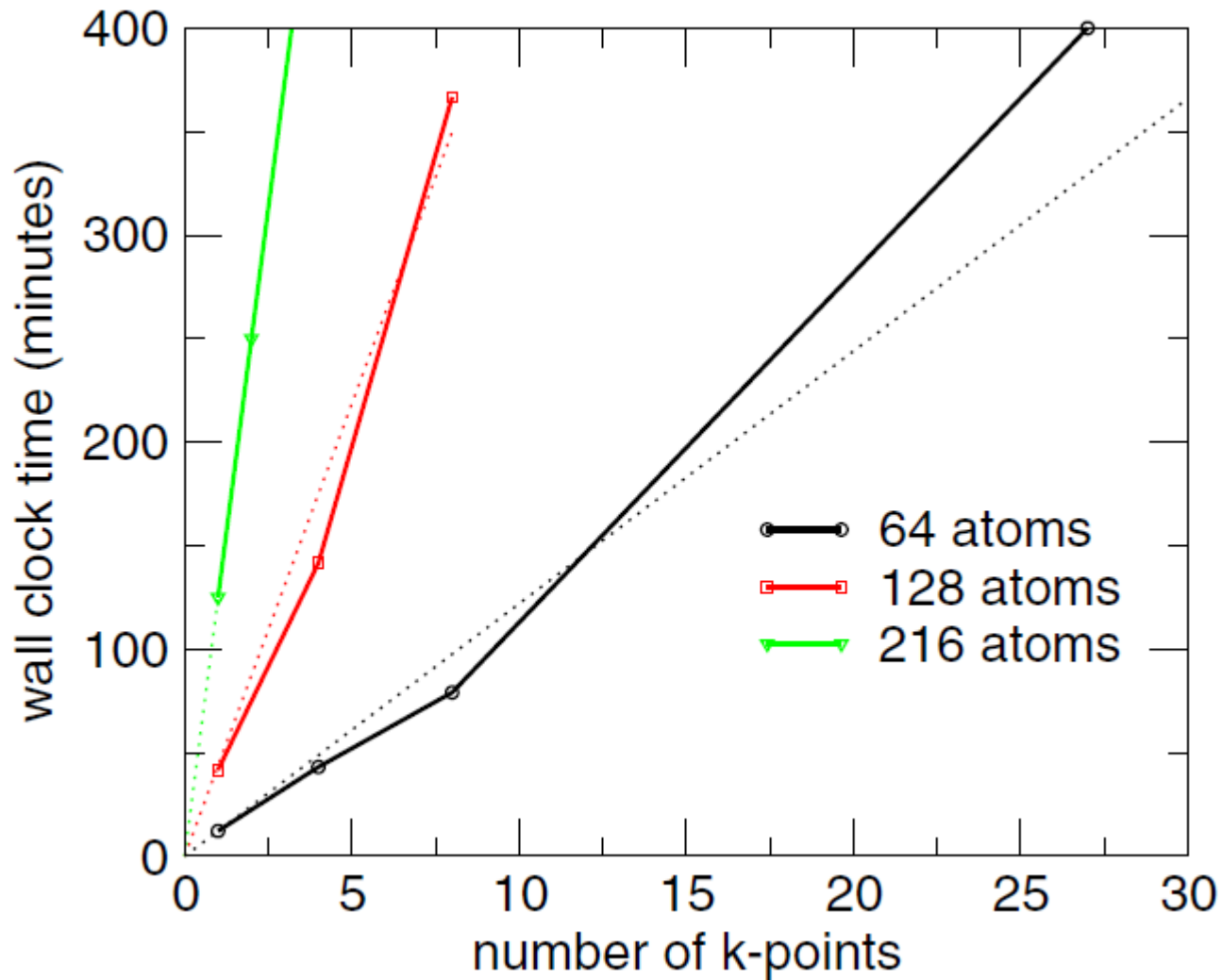
# Cubic scaling in the #atoms

TABLE I. Timings in minutes for an RPA calculation for different bulk Si bcc cells. The calculations are done for the  $\Gamma$  point only and the number of cores is increased with system size. Since one of the computational steps scales only quadratically with system size, the total scaling is better than cubic.

Atoms	Cores	Time	Time $\times$ cores / atoms <sup>3</sup> $\times 10^3$
54	32	14.3	2.91
128	64	83.2	2.54
250	128	299.9	2.45

PHYSICAL REVIEW B **90**, 054115 (2014)

# Linear scaling in #k-points



PHYSICAL REVIEW B **90**, 054115 (2014)

# Formation energies of defects in Si

216 atom	$\Gamma$	2	4	PBE	RPA	HSE +vdW
X(PBE)	3.256	3.341	3.571	3.566		
X	0.724	0.710	0.632	3.566	4.20	4.41
C <sub>3v</sub>	0.820	0.812	0.743	3.619	4.36	4.40
H	0.789	0.779	0.707	3.626	4.33	
T	1.105	1.144	1.139	3.791	4.93	4.51
VJT	0.789	0.755	0.742	3.646	4.39	4.38
256 atom	$\Gamma$	2		PBE	RPA	
VJT(PBE)	3.272	3.518		3.589		
VJT	0.839	0.745		3.589	4.33	

The End

Thank you!